Random vibration analysis of train-slab track-bridge coupling system under earthquakes

Zhi-ping Zeng[*1,2,3], Xian-feng He[1], Yan-gang Zhao[1,2], Zhi-wu Yu[1,3], Ling-kun Chen[3,4], Wen-tao Xu[3,5] and Ping Lou[1,3]

[1]*School of Civil Engineering, Railway Campus, Central South University, 22 Shao-shan-nan Road, Changsha, Hunan 410075, China*
[2]*Department of Architecture, Kanagawa University, 3-27-1 Rokkakubashi, Kanagawa-Ku, Yokohama-shi, Kanagawa, 221-8686, Japan*
[3]*National Engineering Laboratory for High-Speed Railway Construction, Central South University, 22 Shao-shan-nan Road, Changsha, Hunan 410075, China*
[4]*College of civil science and technology, Yangzhou University, 88 Yang-zhou-da-xue-nan Road, Yangzhou, Jiangsu 225127, China*
[5]*School of Mechanics and Engineering Science, Zhengzhou University, 100 Ke-xue Road, Zhengzhou, Henan 450001, China*

Abstract.   This study aimed to investigate the random vibration characteristic of train-slab track-bridge interaction system subjected to both track irregularities and earthquakes by use of pseudo-excitation method (PEM). Each vehicle subsystem was modeled by multibody dynamics. A three-dimensional rail-slab-girder-pier finite element model was created to simulate slab track and bridge subsystem. The equations of motion for the entire system were established based on the constraint condition of no jump between wheel and rail. The random load vectors of equations of motion were formulated by transforming track irregularities and seismic accelerations into a series of deterministic pseudo-excitations according to their respective power spectral density (PSD) functions by means of PEM. The time-dependent PSDs of random vibration responses of the system were obtained by step-by-step integration method, and the corresponding extreme values were estimated based on the first-passage failure criterion. As a case study, an ICE3 high-speed train passing a fifteen-span simply supported girder bridge simultaneously excited by track irregularities and earthquakes is presented. The evaluated extreme values and the PSD characteristic of the random vibration responses of bridge and train are analyzed, and the influences of train speed and track irregularities (without earthquakes) on the random vibration characteristic of bridge and train are discussed.

Keywords: train-slab track-bridge interaction; random vibration; pseudo-excitation method; earthquake; track irregularity

1. Introduction

∗Corresponding author, Ph.D., E-mail: hzzp7475@126.com

High-speed railway has become one of the most important forms of public transportation in many countries (Ju and Li 2011). Meanwhile, bridges have been widely used as the supporting structures for high-speed railway (Zhang *et al*. 2010a). Thus, the dynamic response characteristic of high-speed train passing bridge has been an issue of great concern (Zhai and Cai 2002, Wu and Yang 2003, Xia and Zhang 2005), especially in earthquake-prone regions (Yang and Wu 2002, Sogabe *et al*. 2007, Yau 2009, Du *et al*. 2012, Antolín *et al*. 2013). However, the efforts to study the random vibration characteristic of train-track/bridge shaken by earthquakes are still relatively few (Michal and Michael 2009). Miyamoto *et al*. (1997) have analyzed analytically the operation safety of railway vehicles under the action of earthquakes using a three-dimensional simplified vehicle model, where sine waves are used as the input excitation. Yang *et al*. (2004) have investigated the dynamic stability of trains, initially static or traveling over bridges shaken by earthquakes. In their works, the maximum allowable speed for the train to run safely under four specific seismic accelerations are evaluated. Xia *et al*. (2006) have established a dynamic model of coupled train-bridge system subjected to earthquakes considering the non-uniform characteristics of the seismic wave. Through input of typical seismic waves with different propagation velocities to the train-bridge system, the histories of the train running through the bridge are simulated and the dynamic responses of the bridge and the vehicles are calculated. Frýba and Yau (2009) have studied the effect of various lags of the earthquake arrival on the vibration of long-span suspended bridges. The results indicate that the interaction of both the moving load and the seismic forces may substantially amplify the response of long-span suspended bridges in the vicinity of the supports. Ju (2013) has investigated some improvements of bridge structure, such as the gap between two simply supported girders, pier stiffness and so on, to increase the safety of moving trains during earthquakes using finite element method (FEM). In the aforementioned work, most researchers either ignore the track system or only take the conventional ballasted track into account. With the wide use of slab ballastless track in modern high-speed and urban railway (Gao *et al*. 2006, Li *et al*. 2010, Zhang *et al.* 2014), it becomes more and more necessary to investigate the dynamic responses of train-slab track-bridge interaction system shaken by earthquakes. On the other hand, the track irregularities and seismic motions are usually only treated as one or few time-history samples to compute the random dynamic responses of train-track/bridge interaction system in most of the previous researches. In fact, these results can only be regarded as the particular cases of a sequence of possible outcomes because of the randomness of track irregularities and seismic motion. Therefore it is of great importance to evaluate the dynamic responses of train-track/bridge interaction system on a random vibration basis in order to ensure the reliability of the simulation (Yang *et al*. 2004). Unfortunately, the conventional approach for random vibration analysis (Nigam 1983) is computationally inefficient, especially for the sophisticated train-slab track-bridge interaction system. Therefore more efficient and accurate algorithm should be employed to analyze the random vibration of train-slab track-bridge interaction system, such as PEM (Lin *et al*. 1994, Lu *et al*. 2006, Lu *et al*. 2009). Zhang *et al*. (2010a) have investigated the random vibration for train-bridge system subjected to horizontal earthquake by PEM. However, the track is omitted and the wheel displacements are assumed to be fully constrained by girder displacements and track irregularities, that is to say, the inherent creepage between wheel and rail is not taken into consideration.

In present paper, the three-dimensional characteristic of the train-slab track-bridge system, together with assumptions made for modeling such a system, is first summarized. A three-dimensional train-slab track-bridge interaction model is then constructed based on these assumptions. Next, the equations of motion for the major components of model, i.e., the vehicle,

rail, slab, bridge girder and pier, are formulated by means of FEM and energy principle (Lou and Zeng 2005), and based on which the equations of motion for the entire train-slab track-bridge interaction system are assembled. The track irregularities are regarded as a series of uniformly modulated, multi-point, different-phase random excitations by taking time lags between the wheels into account, while the earthquakes are assumed as a series of uniformly modulated, non-stationary, evolutionary random excitations. Hence the random excitations caused by track irregularities and earthquakes are then transformed into a series of deterministic pseudo-harmonic excitation vectors according to PEM and wheel-rail interaction relationship, so that time-dependent PSDs of the random vibration responses of the entire system excited by track irregularities and earthquakes can be obtained by step-by-step integration method such as Wilson-θ method. A numerical example is presented. Firstly, the reliability and efficiency of PEM for calculating the extreme values of the random dynamic responses of the train-slab track-bridge interaction system is studied through comparison with Monte Carlo method (MCM). Secondly, the PSD characteristic of the random dynamic responses of bridge and train are analyzed. Thirdly, the influence of train speed on the random vibration characteristic of bridge and train are studied. Fourthly, the random vibration characteristic of bridge and train with only track irregularities considered are investigated. Finally, some useful conclusions are drawn.
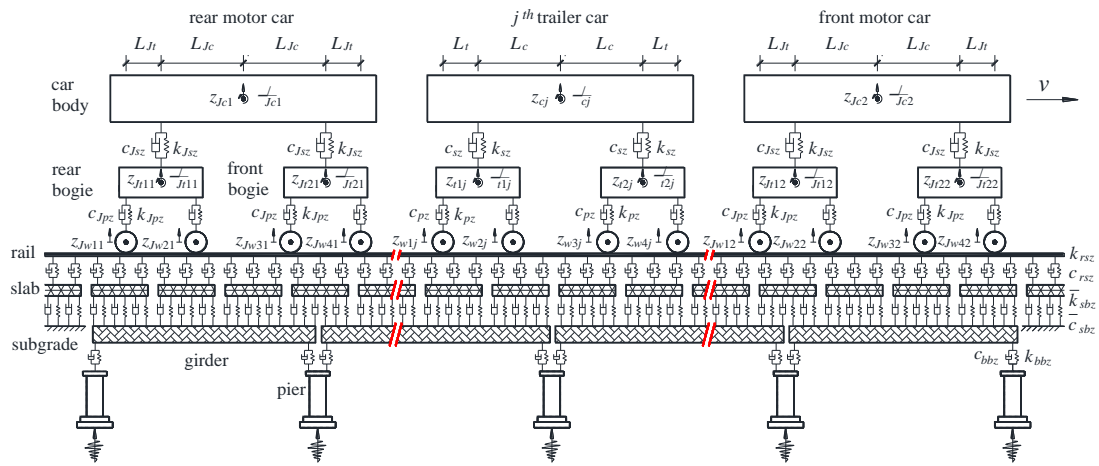
2. Models of train, slab track and bridge

Fig. 1 depicts a train consisting of a series of four-axle vehicles moving with constant speed v on a slab track resting on a simply supported girder bridge shaken by earthquakes. For the sake of simplicity, it is assumed that no inelastic deformation occurs on each subsystem during earthquakes.

2.1 Model of train

The train consists of the rear and front motor cars numbered 1 and 2 respectively, and N_v trailer cars numbered 1, 2, …, N_v from left to right.

Each trailer car in the train is modeled as a mass-spring-damper system consisting of one carbody, two bogies, four wheelsets and two-stage suspensions. As shown in Fig. 1, the carbody rests on the front and rear bogies, each of which in turn is supported by two wheelsets. The carbody is modeled as a rigid body with a mass m_c and three moments of inertia I_{cx}, I_{cy}, I_{cz} about the longitudinal axis x, lateral axis y and vertical axis z through its center of gravity. Similarly, each bogie is considered as a rigid body having a mass m_t and three moments of inertia I_{tx}, I_{ty}, I_{tz}. Each wheelset is considered as a rigid body having a mass m_w and two moments of inertia I_{wx}, I_{wz}. The secondary suspension between carbody and each bogie is characterized by longitudinal spring stiffness k_{sx} and damping coefficient c_{sx}, lateral spring stiffness k_{sy} and damping coefficient c_{sy}, vertical spring stiffness k_{sz} and damping coefficient c_{sz}, respectively. Likewise the spring and shock absorber in the primary suspension for each wheelset are characterized by k_{px} and c_{px}, k_{py} and c_{py}, k_{pz} and c_{pz}, respectively. By neglecting of the longitudinal displacement, the motions of the jth trailer carbody may be described by the lateral displacement y_{cj}, vertical displacement z_{cj}, rolling displacement θ_{cj}, pitching displacement φ_{cj} and yawing displacement ψ_{cj} with respect to its center of gravity, where the subscript j denotes the trailer car number. Similarly, the motions of both the rear and front bogies of the jth trailer car may be also described, respectively, by lateral

displacement y_{t1j} and y_{t2j}, vertical displacement z_{t1j} and z_{t2j}, rolling displacement θ_{t1j} and θ_{t2j}, pitching displacement φ_{t1j} and φ_{t2j}, yawing displacement ψ_{t1j} and ψ_{t2j}. The motions of the four wheelsets from left to right of the *j*th trailer car may be described by lateral displacement y_{w1j}, y_{w2j}, y_{w3j} and y_{w4j}, vertical displacement z_{w1j}, z_{w2j}, z_{w3j} and z_{w4j}, rolling displacement θ_{w1j}, θ_{w2j}, θ_{w3j} and θ_{w4j}, yawing displacement ψ_{w1j}, ψ_{w2j}, ψ_{w3j} and ψ_{w4j}, respectively. Therefore, the total number of DOFs for each trailer car is 31. However, it is assumed that no jump occurs between each wheel of all vehicles and rail in this article, that is, the vertical displacement of wheel is determined by the vertical displacement of rail, while the rolling movement of wheel is determined by the relative lateral movement between the wheel and rail. Consequently, the independent DOFs for each trailer car become 23.
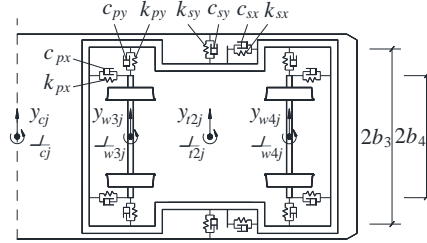

(a) Frontal view
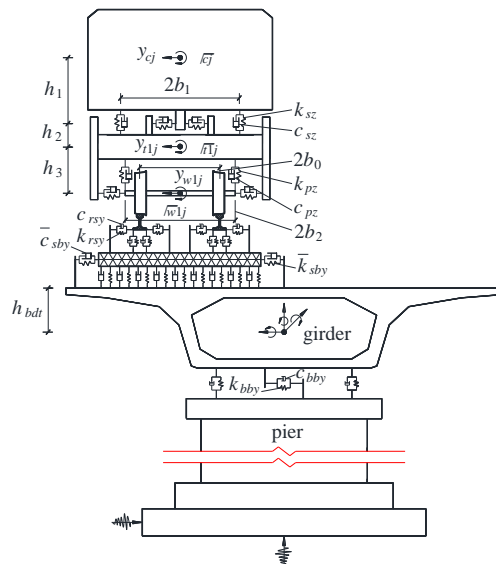
(b) Left side view

Fig. 1 Three-dimensional model for train-slab track-bridge interaction system

(c) Top view (without track and bridge)

Fig. 1 Continued

Each motor car in the train is also modeled as a mass-spring-damper system consisting of a carbody, two bogies, four wheelsets and two-stage suspensions with different physical properties. The carbody has a mass m_{Jc} and three moments of inertia I_{Jcx}, I_{Jcy}, I_{Jcz}. Each bogie has a mass m_{Jt} and three moments of inertia I_{tx}, I_{ty}, I_{tz}. Each wheelset has a mass m_{Jw} and two moments of inertia I_{Jwx}, I_{Jwz}. The secondary suspension is characterized by spring stiffness k_{Jsx}, k_{Jsy}, k_{Jsz} and damping coefficient c_{Jsx}, c_{Jsy}, c_{Jsz}. The primary suspension is characterized by spring stiffness k_{Jpx}, k_{Jpy}, k_{Jpz} and damping coefficient c_{Jpx}, c_{Jpy}, c_{Jpz}. The independent DOFs for each motor car are also 23. The DOFs of carbody are denoted as y_{Jci}, z_{Jci}, θ_{Jci}, φ_{Jci} and ψ_{Jci}. The DOFs of the rear bogie are denoted as y_{Jt1i}, z_{Jt1i}, θ_{Jt1i}, φ_{Jt1i} and ψ_{Jt1i}. The DOFs of the front bogie are denoted as y_{Jt2i}, z_{Jt2i}, θ_{Jt2i}, φ_{Jt2i} and ψ_{Jt2i}. The DOFs of the four wheelsets are denoted as $y_{Jw1i} \sim y_{Jw4i}$, and $\psi_{Jw1i} \sim \psi_{Jw4i}$. Herein the subscript i denotes the motor car number.

2.2 Models of slab track and bridge

As shown in Fig. 1, the rail, slab, bridge girder and pier are all modeled as elastic Bernoulli-Euler beam. On the basis of FEM, the rail, slab, bridge girder and pier are all divided into a series of beam elements of length l. The lateral elasticity and damping properties of the fastener are represented by discrete massless springs with stiffness k_{rsy} and dampers with damping coefficient c_{rsy}. The vertical elasticity and damping properties of the fastener are represented by k_{rsz} and c_{rsz}. The lateral elasticity and damping properties of the CA layer beneath the slab are represented by continuous massless springs with stiffness $\bar{k}_{sby}$ and dampers with damping coefficient $\bar{c}_{sby}$. The vertical elasticity and damping properties of the CA layer are represented by $\bar{k}_{sbz}$ and $\bar{c}_{sbz}$. The elasticity and damping properties of the bridge bearing are represented by massless springs with stiffness k_{bby}, k_{bbz}, $k_{bb\theta}$ and dampers with damping coefficient c_{bby}, c_{bbz}, $c_{bb\theta}$. In addition, the assumption of Rayleigh damping is adopted (Wu and Yang 2003). By neglecting the displacement along x axis, each node of rail, slab and bridge girder has five DOFs, i.e., lateral displacement, vertical displacement, and rotations about x, y and z axes. Each node of pier has three DOFs, i.e., lateral displacement, vertical displacement, and rotation about x axis.

3. Equations of motion for train-slab track-bridge interaction system

By using the energy principle (Lou and Zeng 2005), one can derive the three-dimensional equations of motion written in sub-matrix for the train-slab track-bridge interaction system as

$$
\begin{bmatrix}
\mathbf{M}_{tt} & 0 & 0 & 0 & 0 \\
0 & \mathbf{M}_{rr} & 0 & 0 & 0 \\
0 & 0 & \mathbf{M}_{ss} & 0 & 0 \\
0 & 0 & 0 & \mathbf{M}_{bb} & 0 \\
0 & 0 & 0 & 0 & \mathbf{M}_{pp}
\end{bmatrix}
\begin{bmatrix}
\ddot{\mathbf{X}}_t \\
\ddot{\mathbf{X}}_r \\
\ddot{\mathbf{X}}_s \\
\ddot{\mathbf{X}}_b \\
\ddot{\mathbf{X}}_p
\end{bmatrix}
+
\begin{bmatrix}
\mathbf{C}_{tt} & \mathbf{C}_{tr} & 0 & 0 & 0 \\
\mathbf{C}_{rt} & \mathbf{C}_{rr} & \mathbf{C}_{rs} & 0 & 0 \\
0 & \mathbf{C}_{sr} & \mathbf{C}_{ss} & \mathbf{C}_{sb} & 0 \\
0 & 0 & \mathbf{C}_{bs} & \mathbf{C}_{bb} & \mathbf{C}_{bp} \\
0 & 0 & 0 & \mathbf{C}_{pb} & \mathbf{C}_{pp}
\end{bmatrix}
\begin{bmatrix}
\dot{\mathbf{X}}_t \\
\dot{\mathbf{X}}_r \\
\dot{\mathbf{X}}_s \\
\dot{\mathbf{X}}_b \\
\dot{\mathbf{X}}_p
\end{bmatrix}
+
\begin{bmatrix}
\mathbf{K}_{tt} & \mathbf{K}_{tr} & 0 & 0 & 0 \\
\mathbf{K}_{rt} & \mathbf{K}_{rr} & \mathbf{K}_{rs} & 0 & 0 \\
0 & \mathbf{K}_{sr} & \mathbf{K}_{ss} & \mathbf{K}_{sb} & 0 \\
0 & 0 & \mathbf{K}_{bs} & \mathbf{K}_{bb} & \mathbf{K}_{bp} \\
0 & 0 & 0 & \mathbf{K}_{pb} & \mathbf{K}_{pp}
\end{bmatrix}
\begin{bmatrix}
\mathbf{X}_t \\
\mathbf{X}_r \\
\mathbf{X}_s \\
\mathbf{X}_b \\
\mathbf{X}_p
\end{bmatrix}
=
\begin{bmatrix}
\mathbf{F}_t \\
\mathbf{F}_r \\
\mathbf{F}_s \\
\mathbf{F}_b \\
\mathbf{F}_p
\end{bmatrix}
\tag{1}
$$

where the subscripts 't', 'r', 's', 'b' and 'p' denote the train, rail, slab, bridge girder and pier, respectively. The displacement vector, mass matrix, stiffness matrix, damping matrix, and the load vector of the train, rail, slab, bridge girder and pier are explained briefly as follows, and the detailed derivation can refer to Lou and Zeng (2005).

3.1 Displacement vectors

The total train displacement vector $\mathbf{X}_t$ with order T_{dof} ($T_{dof} = 23 \times N_v + 23 \times 2$) can be written as

$$
\mathbf{X}_t = [\mathbf{X}_{J1} \quad \mathbf{X}_{v1} \quad \mathbf{X}_{v2} \quad \cdots \quad \mathbf{X}_{vN_v} \quad \mathbf{X}_{J2}]^{\mathbf{T}}
\tag{2}
$$

where the superscript '$\mathbf{T}$' denotes the transpose of the matrix, $\mathbf{X}_{vj}$ ($j = 1, 2, \ldots, N_v$) and $\mathbf{X}_{Ji}$ ($i = 1, 2$) are the displacement vectors of the jth trailer car and the ith motor car, respectively, which can be expressed as

$$
\mathbf{X}_{vj} = [y_{cj} \quad z_{cj} \quad \theta_{cj} \quad \varphi_{cj} \quad \psi_{cj} \quad y_{t1j} \quad z_{t1j} \quad \theta_{t1j} \quad \varphi_{t1j} \quad \psi_{t1j} \quad y_{t2j} \quad z_{t2j}
$$

$$
\theta_{t2j} \quad \varphi_{t2j} \quad \psi_{t2j} \quad y_{w1j} \quad \psi_{w1j} \quad y_{w2j} \quad \psi_{w2j} \quad y_{w3j} \quad \psi_{w3j} \quad y_{w4j} \quad \psi_{w4j}]
$$

$$
\mathbf{X}_{Ji} = [y_{Jci} \quad z_{Jci} \quad \theta_{Jci} \quad \varphi_{Jci} \quad \psi_{Jci} \quad y_{Jt1i} \quad z_{Jt1i} \quad \theta_{Jt1i} \quad \varphi_{Jt1i} \quad \psi_{Jt1i} \quad y_{Jt2i} \quad z_{Jt2i}
$$

$$
\theta_{Jt2i} \quad \varphi_{Jt2i} \quad \psi_{Jt2i} \quad y_{Jw1i} \quad \psi_{Jw1i} \quad y_{Jw2i} \quad \psi_{Jw2i} \quad y_{Jw3i} \quad \psi_{Jw3i} \quad y_{Jw4i} \quad \psi_{Jw4i}]
$$

The displacement vector of rail $\mathbf{X}_r$ with order $2N_r \times 1$, comprising displacement vector $\mathbf{X}_{Lr}$ of left rail with order $N_r \times 1$ and displacement vector $\mathbf{X}_{Rr}$ of right rail with order $N_r \times 1$, can be written as

$$
\mathbf{X}_r = [\mathbf{X}_{Lr} \quad \mathbf{X}_{Rr}]^{\mathbf{T}}
$$

$$
\mathbf{X}_{Lr} = \mathbf{X}_{Rr} = [q_{r1} \quad q_{r2} \quad \cdots \quad q_{rN_r}]
\tag{3}
$$

where N_r denotes the total number of DOFs of each rail.

The displacement vector $\mathbf{X}_s$ with order $\bar{N}_s \times 1$ for a series of continuously supported beams to model slabs can be written as

$$
\mathbf{X}_s = [\mathbf{X}_{s1} \quad \mathbf{X}_{s2} \quad \cdots \quad \mathbf{X}_{sN_s}]^{\mathbf{T}}
\tag{4}
$$

where $\mathbf{X}_{si}$ ($i = 1, 2, \ldots, N_s$) denotes the displacement vector of the ith slab, N_s denotes the total number of slabs, and $\bar{N}_s$ denotes the total number of DOFs of all slabs. $\mathbf{X}_{si}$ with order $1 \times \bar{n}_{si}$ and $\bar{N}_s$ can be expressed as

$$
\mathbf{X}_{si} = [q_{s1} \quad q_{s2} \quad \cdots \quad q_{s\bar{n}_{si}}]
$$

$$
\bar{N}_s = \sum_{i=1}^{N_s} \bar{n}_{si}
$$

where $\bar{n}_{si}$ denotes the total number of DOFs of the ith slab.

The displacement vector $\mathbf{X}_b$ with order $\bar{N}_b \times 1$ for a series of simply supported beams to model the bridge girders can be written as

$$\mathbf{X}_b = [\mathbf{X}_{b1} \quad \mathbf{X}_{b2} \quad \cdots \quad \mathbf{X}_{bN_b}]^{\mathbf{T}} \tag{5}$$

where $\mathbf{X}_{bi}$ ($i = 1, 2, \ldots, N_b$) denotes the displacement vector of the ith bridge girder, N_b denotes the total number of bridge girders, and $\bar{N}_b$ denotes the total number of DOFs of all bridge girders. $\mathbf{X}_{bi}$ with order $1 \times \bar{n}_{bi}$ and $\bar{N}_b$ can be expressed as

$$\mathbf{X}_{bi} = [q_{b1} \quad q_{b2} \quad \cdots \quad q_{b\bar{n}_{bi}}]$$

$$\bar{N}_b = \sum_{i=1}^{N_b} \bar{n}_{bi}$$

where $\bar{n}_{bi}$ denotes the total number of DOFs of the ith bridge girder.

The displacement vector of piers $\mathbf{X}_p$ with order $\bar{N}_p \times 1$ can be written as

$$\mathbf{X}_p = [\mathbf{X}_{p1} \quad \mathbf{X}_{p2} \quad \cdots \quad \mathbf{X}_{pN_p}]^{\mathbf{T}} \tag{6}$$

where $\mathbf{X}_{pi}$ ($i = 1, 2, \ldots, N_p$) denotes the displacement vector of the ith pier, N_p denotes the total number of piers, and $\bar{N}_p$ denotes the total number of DOFs of all piers. $\mathbf{X}_{pi}$ with order $1 \times \bar{n}_{pi}$ and $\bar{N}_p$ can be expressed as

$$\mathbf{X}_{pi} = [q_{p1} \quad q_{p2} \quad \cdots \quad q_{p\bar{n}_{pi}}]$$

$$\bar{N}_p = \sum_{i=1}^{N_p} \bar{n}_{pi}$$

where $\bar{n}_{pi}$ denotes the total number of DOFs of the ith pier.

3.2 Matrices for train

The matrices of train are marked with the subscript 'tt'. The mass matrix $\mathbf{M}_{tt}$ of train, with order $(23 \times N_v + 23 \times 2) \times (23 \times N_v + 23 \times 2)$, can be written as

$$\mathbf{M}_{tt} = \text{diag}[\mathbf{M}_{J1} \quad \mathbf{M}_{v1} \quad \mathbf{M}_{v2} \quad \cdots \quad \mathbf{M}_{vN_v} \quad \mathbf{M}_{J2}] \tag{7}$$

where $\mathbf{M}_{vj}$ and $\mathbf{M}_{Ji}$ with order 23×23 denote the mass matrices of the jth trailer car and ith motor car, respectively, and can be expressed as

$$\mathbf{M}_{vj} = \text{diag}[m_c \quad m_c \quad I_{cx} \quad I_{cy} \quad I_{cz} \quad m_t \quad m_t \quad I_{tx} \quad I_{ty} \quad I_{tz} \quad m_t \quad m_t$$

$$I_{tx} \quad I_{ty} \quad I_{tz} \quad m_w \quad I_{wz} \quad m_w \quad I_{wz} \quad m_w \quad I_{wz} \quad m_w \quad I_{wz}]$$

$$\mathbf{M}_{Ji} = \text{diag}[m_{Jc} \quad m_{Jc} \quad I_{Jcx} \quad I_{Jcy} \quad I_{Jcz} \quad m_{Jt} \quad m_{Jt} \quad I_{Jtx} \quad I_{Jty} \quad I_{Jtz} \quad m_{Jt} \quad m_{Jt}$$

$$I_{Jtx} \quad I_{Jty} \quad I_{Jtz} \quad m_{Jw} \quad I_{Jwz} \quad m_{Jw} \quad I_{Jwz} \quad m_{Jw} \quad I_{Jwz} \quad m_{Jw} \quad I_{Jwz}]$$

The stiffness matrix $\mathbf{K}_{tt}$ of train, with order $(23 \times N_v + 23 \times 2) \times (23 \times N_v + 23 \times 2)$, can be written as

$$\mathbf{K}_{tt} = \mathrm{diag}[\mathbf{K}_{J1} \quad \mathbf{K}_{v1} \quad \mathbf{K}_{v2} \quad \cdots \quad \mathbf{K}_{vN_v} \quad \mathbf{K}_{J2}] \qquad (8)$$

where $\mathbf{K}_{vj}$ and $\mathbf{K}_{Ji}$ with order 23×23 denote the stiffness matrices of the *j*th trailer car and *i*th motor car.

The damping matrix $\mathbf{C}_{tt}$ of train with order $(23 \times N_v + 23 \times 2) \times (23 \times N_v + 23 \times 2)$, can be obtained by simply replacing *k* in the corresponding stiffness matrix $\mathbf{K}_{tt}$ by *c*.

3.3 Matrices for rail, slab, bridge girder and pier

The matrices of rail are marked with the subscript '*rr*'. The mass matrix $\mathbf{M}_{rr}$ of rail with order $2N_r \times 2N_r$, comprising mass matrix $\mathbf{M}_{Lrr}$ of left rail with order $N_r \times N_r$ and mass matrix $\mathbf{M}_{Rrr}$ of right rail with order $N_r \times N_r$, can be written as

$$\mathbf{M}_{rr} = \mathrm{diag}[\mathbf{M}_{Lrr} \quad \mathbf{M}_{Rrr}] \qquad (9)$$

The stiffness matrix $\mathbf{K}_{rr}$ of rail, with order $2N_r \times 2N_r$, composed of stiffness matrix $\mathbf{K}_{Lrr}$ of left rail with order $N_r \times N_r$, stiffness matrix $\mathbf{K}_{Rrr}$ of right rail with order $N_r \times N_r$, and left rail-right rail interaction stiffness matrices $\mathbf{K}_{LrRr}$ and $\mathbf{K}_{RrLr}$ with order $N_r \times N_r$, can be written as

$$\mathbf{K}_{rr} = \begin{bmatrix} \mathbf{K}_{Lrr} & \mathbf{K}_{LrRr} \\ \mathbf{K}_{RrLr} & \mathbf{K}_{Rrr} \end{bmatrix} \qquad (10)$$

where the stiffness matrices $\mathbf{K}_{LrRr}$ and $\mathbf{K}_{RrLr}$ are induced by the gravity force of train acting upon rails by wheelsets.

The damping matrix $\mathbf{C}_{rr}$ of rail, with order $2N_r \times 2N_r$, consisting of damping matrix $\mathbf{C}_{Lrr}$ of left rail with order $N_r \times N_r$, and damping matrix $\mathbf{C}_{Rrr}$ of right rail with order $N_r \times N_r$, can be written as

$$\mathbf{C}_{rr} = \mathrm{diag}[\mathbf{C}_{Lrr} \quad \mathbf{C}_{Rrr}] \qquad (11)$$

The matrices of slab, bridge girder and pier, marked with the subscript '*ss*', '*bb*' and '*pp*', respectively, are not given here but can be derived by following the similar procedure for derivation of rail matrices.

3.4 Matrices for train-rail interaction

The matrices for the train-rail interaction, marked with subscript '*tr*' or '*rt*', consist of train-left rail interaction matrix marked with subscript '*tLr*', and train-right rail interaction matrix marked with subscript '*tRr*'. The stiffness matrix $\mathbf{K}_{tr}$ and $\mathbf{K}_{rt}$ with order $T_{dof} \times 2N_r$, and damping matrix $\mathbf{C}_{tr}$ and $\mathbf{C}_{rt}$ with order $T_{dof} \times 2N_r$, for train-rail interaction can be written according to the vertical and lateral wheel-rail interaction relationship (Kalker 1967 and Zhang *et al.* 2010b), respectively, as

$$\mathbf{K}_{tr} = [\mathbf{K}_{tLr} \quad \mathbf{K}_{tRr}]_{T_{dof} \times 2N_r} \qquad (12)$$

$$\mathbf{C}_{tr} = [\mathbf{C}_{tLr} \quad \mathbf{C}_{tRr}]_{T_{dof} \times 2N_r}$$

$$\mathbf{K}_{rt} = \mathbf{K}_{tr}^{\mathbf{T}} \qquad \mathbf{C}_{rt} = \mathbf{C}_{tr}^{\mathbf{T}} \qquad (13)$$

where the stiffness matrices $\mathbf{K}_{tLr}$ and $\mathbf{K}_{tRr}$, and the damping matrices $\mathbf{C}_{tLr}$ and $\mathbf{C}_{tRr}$, with order $T_{dof} \times 2N_r$, can be expressed, respectively, as

$$\mathbf{K}_{tLr} = \sum_{j=1}^{N_v} \sum_{h=1}^{4} \mathbf{K}_{v_j-Lr_h}^{V} + \sum_{i=1}^{2} \sum_{h=1}^{4} \mathbf{K}_{J_i-Lr_h}^{V}$$

$$\mathbf{K}_{tRr} = \sum_{j=1}^{N_v} \sum_{h=1}^{4} \mathbf{K}_{v_j-Rr_h}^{V} + \sum_{i=1}^{2} \sum_{h=1}^{4} \mathbf{K}_{J_i-Rr_h}^{V}$$

$$\mathbf{C}_{tLr} = \sum_{j=1}^{N_v} \sum_{h=1}^{4} \mathbf{C}_{v_j-Lr_h}^{V} + \sum_{j=1}^{N_v} \sum_{h=1}^{4} \mathbf{C}_{v_j-Lr_h}^{L} + \sum_{i=1}^{2} \sum_{h=1}^{4} \mathbf{C}_{J_i-Lr_h}^{V} + \sum_{i=1}^{2} \sum_{h=1}^{4} \mathbf{C}_{J_i-Lr_h}^{L}$$

$$\mathbf{C}_{tRr} = \sum_{j=1}^{N_v} \sum_{h=1}^{4} \mathbf{C}_{v_j-Rr_h}^{V} + \sum_{j=1}^{N_v} \sum_{h=1}^{4} \mathbf{C}_{v_j-Rr_h}^{L} + \sum_{i=1}^{2} \sum_{h=1}^{4} \mathbf{C}_{J_i-Rr_h}^{V} + \sum_{i=1}^{2} \sum_{h=1}^{4} \mathbf{C}_{J_i-Rr_h}^{L}$$

in which $\mathbf{K}_{v_j-Lr_h}^{V}$ and $\mathbf{C}_{v_j-Lr_h}^{V}$ represent, respectively, the stiffness and damping matrices induced by the vertical interaction between the *h*th wheelset of the *j*th trailer car and the left rail; $\mathbf{K}_{v_j-Rr_h}^{V}$ and $\mathbf{C}_{v_j-Rr_h}^{V}$ represent, respectively, the stiffness and damping matrices induced by the vertical interaction between the *h*th wheelset of the *j*th trailer car and the right rail; $\mathbf{C}_{v_j-Lr_h}^{L}$ and $\mathbf{C}_{v_j-Rr_h}^{L}$ represent, respectively, the damping matrices induced by the lateral interaction between the *h*th wheelset of the *j*th trailer car and the left and right rails. Similarly, $\mathbf{K}_{J_i-Lr_h}^{V}$, $\mathbf{K}_{J_i-Rr_h}^{V}$, $\mathbf{C}_{J_i-Lr_h}^{V}$, $\mathbf{C}_{J_i-Rr_h}^{V}$, $\mathbf{C}_{J_i-Lr_h}^{L}$ and $\mathbf{C}_{J_i-Rr_h}^{L}$ represent, respectively, the stiffness and damping matrices induced by the interaction between the *i*th motor car and the left and right rails.

3.5 Matrices for rail-slab interaction

The matrices for rail-slab interaction, marked with subscript '*rs*' or '*sr*', consist of left rail-slab interaction matrix marked with subscript '*Lrs*', and right rail-slab interaction matrix marked with subscript '*Rrs*'. The stiffness matrix $\mathbf{K}_{rs}$ with order $2N_r \times \bar{N}_s$ induced by the stiffness k_{rsy} and k_{rsz} of fastener between rail and slab can be written as

$$\mathbf{K}_{rs} = \begin{bmatrix} \mathbf{K}_{Lrs} \\ \mathbf{K}_{Rrs} \end{bmatrix}_{2N_r \times \bar{N}_s}$$

$$\mathbf{K}_{sr} = \mathbf{K}_{rs}^{\mathbf{T}} \tag{14}$$

The damping matrix $\mathbf{C}_{rs}$ with order $2N_r \times \bar{N}_s$ can be obtained by replacing k_{rsy} and k_{rsz} in the corresponding stiffness matrix $\mathbf{K}_{rs}$ by c_{rsy} and c_{rsz}. Similarly, one also has $\mathbf{C}_{sr} = \mathbf{C}_{rs}^{\mathbf{T}}$.

3.6 Matrices for slab-girder interaction

The matrices for slab-girder interaction are marked with subscript '*sb*' or '*bs*'. The stiffness matrix $\mathbf{K}_{sb}$ with order $\bar{N}_s \times \bar{N}_b$ induced by the stiffness $\bar{k}_{sby}$ and $\bar{k}_{sbz}$ of CA layer between slab and bridge girder can be written as

$$\mathbf{K}_{sb} = \text{diag}[\mathbf{K}_{sb1} \quad \mathbf{K}_{sb2} \quad \cdots \quad \mathbf{K}_{sbN_b}] \tag{15}$$

where $\mathbf{K}_{sbi}$ ($i = 1, 2, \ldots, N_b$) denotes the stiffness matrix induced by the stiffness of CA layer lying between the *i*th bridge girder and all the corresponding slab.

Similarly, the damping matrix $\mathbf{C}_{sb}$ with order $\bar{N}_s \times \bar{N}_b$ can be obtained by replacing $\bar{k}_{sby}$ and $\bar{k}_{sbz}$ in the corresponding stiffness matrix $\mathbf{K}_{sb}$ by $\bar{c}_{sby}$ and $\bar{c}_{sbz}$. One can have $\mathbf{K}_{bs} = \mathbf{K}_{sb}^{\mathbf{T}}$ and $\mathbf{C}_{bs} = \mathbf{C}_{sb}^{\mathbf{T}}$.

3.7 Matrices for girder-pier interaction

The matrices induced by stiffness and damping of bearing between bridge girder and pier are marked with subscript '*bp*' or '*pb*'. The stiffness matrix $\mathbf{K}_{bp}$ with order $\bar{N}_b \times \bar{N}_p$ can be derived by the stiffness of bearing. Similarly, the damping matrix $\mathbf{C}_{bp}$ with order $\bar{N}_b \times \bar{N}_p$ can be obtained by the damping of bearing. One also has $\mathbf{K}_{pb} = \mathbf{K}_{bp}^{\mathbf{T}}$ and $\mathbf{C}_{pb} = \mathbf{C}_{bp}^{\mathbf{T}}$.

3.8 Load vector for train, rail, slab, girder and pier

The load vector $\mathbf{F}_t$ of train with order $T_{dof} \times 1$ can be written as

$$\mathbf{F}_t = [\mathbf{F}_t^1 \ \mathbf{F}_t^2]^{\mathbf{T}}$$

$$\mathbf{F}_t^1 = [\mathbf{F}_{J1}^1 \ \mathbf{F}_{v1}^1 \ \mathbf{F}_{v2}^1 \ \dots \ \mathbf{F}_{vN_v}^1 \ \mathbf{F}_{J2}^1]^{\mathbf{T}} \qquad \mathbf{F}_t^2 = [\mathbf{F}_{J1}^2 \ \mathbf{F}_{v1}^2 \ \mathbf{F}_{v2}^2 \ \dots \ \mathbf{F}_{vN_v}^2 \ \mathbf{F}_{J2}^2]^{\mathbf{T}} \tag{16}$$

where the load vector of the *j*th trailer car $\mathbf{F}_{vj}^1$ and $\mathbf{F}_{vj}^2$, and the load vector of the *i*th motor car $\mathbf{F}_{Ji}^1$ and $\mathbf{F}_{Ji}^2$, with order 23×1 can be written, respectively, as

$$\mathbf{F}_{vj}^1 = \left\{ \begin{array}{c} 0 \\ 0 \\ 0 \\ 0 \\ 0 \\ 0 \\ k_{pz}[2r(x_{j1}^V) + 2r(x_{j2}^V)] \\ k_{pz}b_2[r(x_{j1}^C) + r(x_{j2}^C)] \\ k_{pz}L_t[2r(x_{j1}^V) - 2r(x_{j2}^V)] \\ 0 \\ 0 \\ k_{pz}[2r(x_{j3}^V) + 2r(x_{j4}^V)] \\ k_{pz}b_2[r(x_{j3}^C) + r(x_{j4}^C)] \\ k_{pz}L_t[2r(x_{j3}^V) - 2r(x_{j4}^V)] \\ 0 \\ \frac{W_{axle}\lambda}{b_0}r(x_{j1}^A) \\ 0 \\ \frac{W_{axle}\lambda}{b_0}r(x_{j2}^A) \\ 0 \\ \frac{W_{axle}\lambda}{b_0}r(x_{j3}^A) \\ 0 \\ \frac{W_{axle}\lambda}{b_0}r(x_{j4}^A) \\ 0 \end{array} \right\}^{\mathbf{T}} \qquad \mathbf{F}_{Ji}^1 = \left\{ \begin{array}{c} 0 \\ 0 \\ 0 \\ 0 \\ 0 \\ 0 \\ k_{Jpz}[2r(x_{Ji1}^V) + 2r(x_{Ji2}^V)] \\ k_{Jpz}b_{J2}[r(x_{Ji1}^C) + r(x_{Ji2}^C)] \\ k_{Jpz}L_{Jt}[2r(x_{Ji1}^V) - 2r(x_{Ji2}^V)] \\ 0 \\ 0 \\ k_{Jpz}[2r(x_{Ji3}^V) + 2r(x_{Ji4}^V)] \\ k_{Jpz}b_{J2}[r(x_{Ji3}^C) + r(x_{Ji4}^C)] \\ k_{Jpz}L_{Jt}[2r(x_{Ji3}^V) - 2r(x_{Ji4}^V)] \\ 0 \\ \frac{W_{Jaxle}\lambda_J}{b_{J0}}r(x_{Ji1}^A) \\ 0 \\ \frac{W_{Jaxle}\lambda_J}{b_{J0}}r(x_{Ji2}^A) \\ 0 \\ \frac{W_{Jaxle}\lambda_J}{b_{J0}}r(x_{Ji3}^A) \\ 0 \\ \frac{W_{Jaxle}\lambda_J}{b_{J0}}r(x_{Ji4}^A) \\ 0 \end{array} \right\}^{\mathbf{T}}$$

$$\mathbf{F}_{vj}^2 = \left\{ \begin{array}{c} 0 \\ 0 \\ 0 \\ 0 \\ 0 \\ 0 \\ c_{pz}[2\dot{r}(x_{j1}^V) + 2\dot{r}(x_{j2}^V)] \\ c_{pz}b_2[\dot{r}(x_{j1}^C) + \dot{r}(x_{j2}^C)] \\ c_{pz}L_t[2\dot{r}(x_{j1}^V) - 2\dot{r}(x_{j2}^V)] \\ 0 \\ 0 \\ c_{pz}[2\dot{r}(x_{j3}^V) + 2\dot{r}(x_{j4}^V)] \\ c_{pz}b_2[\dot{r}(x_{j3}^C) + \dot{r}(x_{j4}^C)] \\ c_{pz}L_t[2\dot{r}(x_{j3}^V) - 2\dot{r}(x_{j4}^V)] \\ 0 \\ f_{Lj1}^{22}[\dot{r}(x_{j1}^A) + \frac{1}{2}\dot{r}(x_{j1}^G)] + f_{Rj1}^{22}[\dot{r}(x_{j1}^A) - \frac{1}{2}\dot{r}(x_{j1}^G)] \\ 0 \\ f_{Lj2}^{22}[\dot{r}(x_{j2}^A) + \frac{1}{2}\dot{r}(x_{j2}^G)] + f_{Rj2}^{22}[\dot{r}(x_{j2}^A) - \dot{r}(x_{j2}^G)] \\ 0 \\ f_{Lj3}^{22}[\dot{r}(x_{j3}^A) + \frac{1}{2}\dot{r}(x_{j3}^G)] + f_{Rj3}^{22}[\dot{r}(x_{j3}^A) - \frac{1}{2}\dot{r}(x_{j3}^G)] \\ 0 \\ f_{Lj4}^{22}[\dot{r}(x_{j4}^A) + \frac{1}{2}\dot{r}(x_{j4}^G)] + f_{Rj4}^{22}[\dot{r}(x_{j4}^A) - \frac{1}{2}\dot{r}(x_{j4}^G)] \\ 0 \end{array} \right\}^{\mathbf{T}}$$

$$\mathbf{F}_{Ji}^2 = \left\{ \begin{array}{c} 0 \\ 0 \\ 0 \\ 0 \\ 0 \\ 0 \\ c_{Jpz}[2\dot{r}(x_{Ji1}^V) + 2\dot{r}(x_{Ji2}^V)] \\ c_{Jpz}b_{Jp2}[\dot{r}(x_{Ji1}^C) + \dot{r}(x_{Ji1}^C)] \\ c_{Jpz}L_{Jt}[2\dot{r}(x_{Ji1}^V) - 2\dot{r}(x_{Ji2}^V)] \\ 0 \\ 0 \\ c_{Jpz}[2\dot{r}(x_{Ji3}^V) + 2\dot{r}(x_{Ji4}^V)] \\ c_{Jpz}b_{J2}[\dot{r}(x_{Ji3}^C) + \dot{r}(x_{Ji4}^C)] \\ c_{Jpz}L_{Jt}[2\dot{r}(x_{Ji3}^V) - 2\dot{r}(x_{Ji4}^V)] \\ 0 \\ f_{LJi1}^{22}[\dot{r}(x_{Ji1}^A) + \frac{1}{2}\dot{r}(x_{Ji1}^G)] + f_{RJi1}^{22}[\dot{r}(x_{Ji1}^A) - \frac{1}{2}\dot{r}(x_{Ji1}^G)] \\ 0 \\ f_{LJi2}^{22}[\dot{r}(x_{Ji2}^A) + \frac{1}{2}\dot{r}(x_{Ji2}^G)] + f_{RJi2}^{22}[\dot{r}(x_{Ji2}^A) - \frac{1}{2}\dot{r}(x_{Ji2}^G)] \\ 0 \\ f_{LJi3}^{22}[\dot{r}(x_{Ji3}^A) + \frac{1}{2}\dot{r}(x_{Ji3}^G)] + f_{RJi3}^{22}[\dot{r}(x_{Ji3}^A) - \frac{1}{2}\dot{r}(x_{Ji3}^G)] \\ 0 \\ f_{LJi4}^{22}[\dot{r}(x_{Ji4}^A) + \frac{1}{2}\dot{r}(x_{Ji4}^G)] + f_{RJi4}^{22}[\dot{r}(x_{Ji4}^A) - \frac{1}{2}\dot{r}(x_{Ji4}^G)] \\ 0 \end{array} \right\}^{\mathbf{T}}$$

in which $r(x_{jh}^V)$, $r(x_{jh}^C)$, $r(x_{jh}^A)$ and $r(x_{jh}^G)$ are, respectively, track elevation, cross level, alignment and gauge irregularities at the *h*th wheel-rail contact point of the *j*th trailer car; $r(x_{Jih}^V)$, $r(x_{Jih}^C)$, $r(x_{Jih}^A)$ and $r(x_{Jih}^G)$ are the corresponding track irregularities at the *h*th wheel-rail contact point of the *i*th motor car; $\dot{r}(\cdot)$ is the first derivative of track irregularity $r(\cdot)$; W_{axle} and W_{Jaxle} are the axle weights of trailer and motor car, respectively; λ and λ_J are the slope of the wheel tread of trailer and motor car, respectively; f_{Ljh}^{22} and f_{Rjh}^{22} ($h = 1 \sim 4$) are the lateral creepage coefficients between the *h*th wheelset of the *j*th trailer car and the left and right rails, respectively (Kalker 1967 and Zhang *et al.* 2010b); and f_{LJih}^{22} and f_{RJih}^{22} are the lateral creepage coefficients between the *h*th wheelset of the *i*th motor car and the left and right rails, respectively.

Then, the load vector $\mathbf{F}_t$ of train can be expressed as

$$\mathbf{F}_t = \mathbf{F}_t^{1V} + \mathbf{F}_t^{2V} + \mathbf{F}_t^{1C} + \mathbf{F}_t^{2C} + \mathbf{F}_t^{1A} + \mathbf{F}_t^{2A} + \mathbf{F}_t^{2G} \tag{17}$$

with

$$\mathbf{F}_t^{1V} = [\mathbf{F}_{J1}^{1V} \quad \mathbf{F}_{v1}^{1V} \quad \mathbf{F}_{v2}^{1V} \quad \dots \quad \mathbf{F}_{vN_v}^{1V} \quad \mathbf{F}_{J2}^{1V}]^{\mathbf{T}} \qquad \mathbf{F}_t^{1C} = [\mathbf{F}_{J1}^{1C} \quad \mathbf{F}_{v1}^{1C} \quad \mathbf{F}_{v2}^{1C} \quad \dots \quad \mathbf{F}_{vN_v}^{1C} \quad \mathbf{F}_{J2}^{1C}]^{\mathbf{T}}$$

$$\mathbf{F}_t^{1A} = [\mathbf{F}_{J1}^{1A} \quad \mathbf{F}_{v1}^{1A} \quad \mathbf{F}_{v2}^{1A} \quad \dots \quad \mathbf{F}_{vN_v}^{1A} \quad \mathbf{F}_{J2}^{1A}]^{\mathbf{T}} \qquad \mathbf{F}_t^{2V} = [\mathbf{F}_{J1}^{2V} \quad \mathbf{F}_{v1}^{2V} \quad \mathbf{F}_{v2}^{2V} \quad \dots \quad \mathbf{F}_{vN_v}^{2V} \quad \mathbf{F}_{J2}^{2V}]^{\mathbf{T}}$$

$$\mathbf{F}_t^{2C} = [\mathbf{F}_{J1}^{2C} \quad \mathbf{F}_{v1}^{2C} \quad \mathbf{F}_{v2}^{2C} \quad \dots \quad \mathbf{F}_{vN_v}^{2C} \quad \mathbf{F}_{J2}^{2C}]^{\mathbf{T}} \qquad \mathbf{F}_t^{2A} = [\mathbf{F}_{J1}^{2A} \quad \mathbf{F}_{v1}^{2A} \quad \mathbf{F}_{v2}^{2A} \quad \dots \quad \mathbf{F}_{vN_v}^{2A} \quad \mathbf{F}_{J2}^{2A}]^{\mathbf{T}}$$

$$\mathbf{F}_t^{2G} = [\mathbf{F}_{J1}^{2G} \quad \mathbf{F}_{v1}^{2G} \quad \mathbf{F}_{v2}^{2G} \quad \dots \quad \mathbf{F}_{vN_v}^{2G} \quad \mathbf{F}_{J2}^{2G}]^{\mathbf{T}}$$

where $\mathbf{F}_t^{1V}$, $\mathbf{F}_t^{1C}$ and $\mathbf{F}_t^{1A}$ represent, respectively, the load vectors caused by track elevation,

cross level and alignment irregularities; $\mathbf{F}_t^{2V}$, $\mathbf{F}_t^{2C}$, $\mathbf{F}_t^{2A}$ and $\mathbf{F}_t^{2G}$ represent, respectively, the load vectors caused by the velocity of track elevation, cross level, alignment and gauge irregularities.

The load vector of rail $\mathbf{F}_r$ with order $2N_r \times 1$ can be written as

$$\mathbf{F}_r = \begin{bmatrix} \mathbf{F}_r^L \\ \mathbf{F}_r^R \end{bmatrix}$$

$$\mathbf{F}_r^L = \mathbf{F}_r^{L0} + \mathbf{F}_r^{L1} + \mathbf{F}_r^{L2} + \mathbf{F}_r^{L3} + \mathbf{F}_r^{L4} + \mathbf{F}_r^{L5} + \mathbf{F}_r^{L6} + \mathbf{F}_r^{L7} + \mathbf{F}_r^{L8} + \mathbf{F}_r^{L9} + \mathbf{F}_r^{L10}$$

$$\mathbf{F}_r^R = \mathbf{F}_r^{R0} + \mathbf{F}_r^{R1} + \mathbf{F}_r^{R2} + \mathbf{F}_r^{R3} + \mathbf{F}_r^{R4} + \mathbf{F}_r^{R5} + \mathbf{F}_r^{R6} + \mathbf{F}_r^{R7} + \mathbf{F}_r^{R8} + \mathbf{F}_r^{R9} + \mathbf{F}_r^{R10} \tag{18}$$

where $\mathbf{F}_r^{L0}$, $\mathbf{F}_r^{L1}$, $\mathbf{F}_r^{L2}$, $\mathbf{F}_r^{L3}$ and $\mathbf{F}_r^{L4}$ represent, respectively, the load vectors of each wheelset of train acting upon left rail caused by the gravity force of train, track elevation irregularity, cross level irregularity, alignment irregularity and gauge irregularity; $\mathbf{F}_r^{L5}$, $\mathbf{F}_r^{L6}$, $\mathbf{F}_r^{L7}$ and $\mathbf{F}_r^{L8}$ represent, respectively, the load vectors of each wheelset of train acting upon left rail caused by the velocity of track elevation, cross level, alignment and gauge irregularities; $\mathbf{F}_r^{L9}$ and $\mathbf{F}_r^{L10}$ represent, respectively, the load vectors of the each wheelset of train acting upon left rail caused by the acceleration of track elevation and cross level irregularities. Accordingly, $\mathbf{F}_r^{R0} \sim \mathbf{F}_r^{R10}$ represent, respectively, the load vectors of the each wheelset of train acting upon right rail.

Each element for load vector of slab $\mathbf{F}_s$ with order $\bar{N}_s \times 1$ is zero.

The load vector of bridge girder $\mathbf{F}_b$ with order $\bar{N}_b \times 1$ can be written as

$$\mathbf{F}_b = [\mathbf{F}_{b1} \quad \mathbf{F}_{b2} \quad \cdots \quad \mathbf{F}_{bN_b}]^{\mathbf{T}}$$

$$\mathbf{F}_{bi} = [f_{b1} \quad f_{b2} \quad \cdots \quad f_{bn_{bi}} \quad f_{bn_{bi}+1}] \qquad f_{bi} = [m_{bi}a_{gy} \quad m_{bi}a_{gz} \quad 0 \quad 0 \quad 0] \tag{19}$$

where m_{bi} denotes the mass of node of the ith bridge girder, and a_{gy} and a_{gz} denote, respectively, the lateral horizontal and vertical seismic accelerations.

Similarly the load vector of pier $\mathbf{F}_p$ with order $\bar{N}_p \times 1$ can be written as

$$\mathbf{F}_p = [\mathbf{F}_{p1} \quad \mathbf{F}_{p2} \quad \cdots \quad \mathbf{F}_{pN_p}]^{\mathbf{T}}$$

$$\mathbf{F}_{pi} = [f_{p1} \quad f_{p2} \quad \cdots \quad f_{pn_{pi}} \quad f_{pn_{pi}+1}] \qquad f_{pi} = [m_{pi}a_{gy} \quad m_{pi}a_{gz} \quad 0] \tag{20}$$

where m_{pi} denotes the mass of node of the ith pier.

Now let:

$$\mathbf{F}_{GRT}(t) = \begin{bmatrix} \mathbf{0}_{T_{dof} \times 1} \\ \mathbf{F}_r^{L0} \\ \mathbf{F}_r^{R0} \\ \mathbf{0}_{\bar{N}_s \times 1} \\ \mathbf{0}_{\bar{N}_b \times 1} \\ \mathbf{0}_{\bar{N}_p \times 1} \end{bmatrix} \quad \mathbf{F}_{RND}^1(t) = \begin{bmatrix} \mathbf{F}_t^{1V} \\ \mathbf{F}_r^{L1} \\ \mathbf{F}_r^{R1} \\ \mathbf{0}_{\bar{N}_s \times 1} \\ \mathbf{0}_{\bar{N}_b \times 1} \\ \mathbf{0}_{\bar{N}_p \times 1} \end{bmatrix} \quad \mathbf{F}_{RND}^2(t) = \begin{bmatrix} \mathbf{F}_t^{1C} \\ \mathbf{F}_r^{L2} \\ \mathbf{F}_r^{R2} \\ \mathbf{0}_{\bar{N}_s \times 1} \\ \mathbf{0}_{\bar{N}_b \times 1} \\ \mathbf{0}_{\bar{N}_p \times 1} \end{bmatrix} \quad \mathbf{F}_{RND}^3(t) = \begin{bmatrix} \mathbf{F}_t^{1A} \\ \mathbf{F}_r^{L3} \\ \mathbf{F}_r^{R3} \\ \mathbf{0}_{\bar{N}_s \times 1} \\ \mathbf{0}_{\bar{N}_b \times 1} \\ \mathbf{0}_{\bar{N}_p \times 1} \end{bmatrix}$$

$$\mathbf{F}_{RND}^4(t) = \begin{bmatrix} \mathbf{0}_{T_{dof}\times 1} \\ \mathbf{F}_r^{L4} \\ \mathbf{F}_r^{R4} \\ \mathbf{0}_{\bar{N}_s\times 1} \\ \mathbf{0}_{\bar{N}_b\times 1} \\ \mathbf{0}_{\bar{N}_p\times 1} \end{bmatrix} \quad \mathbf{F}_{RND}^5(t) = \begin{bmatrix} \mathbf{F}_t^{2V} \\ \mathbf{F}_r^{L5} \\ \mathbf{F}_r^{R5} \\ \mathbf{0}_{\bar{N}_s\times 1} \\ \mathbf{0}_{\bar{N}_b\times 1} \\ \mathbf{0}_{\bar{N}_p\times 1} \end{bmatrix} \quad \mathbf{F}_{RND}^6(t) = \begin{bmatrix} \mathbf{F}_t^{2C} \\ \mathbf{F}_r^{L6} \\ \mathbf{F}_r^{R6} \\ \mathbf{0}_{\bar{N}_s\times 1} \\ \mathbf{0}_{\bar{N}_b\times 1} \\ \mathbf{0}_{\bar{N}_p\times 1} \end{bmatrix} \quad \mathbf{F}_{RND}^7(t) = \begin{bmatrix} \mathbf{F}_t^{2A} \\ \mathbf{F}_r^{L7} \\ \mathbf{F}_r^{R7} \\ \mathbf{0}_{\bar{N}_s\times 1} \\ \mathbf{0}_{\bar{N}_b\times 1} \\ \mathbf{0}_{\bar{N}_p\times 1} \end{bmatrix}$$

$$\mathbf{F}_{RND}^8(t) = \begin{bmatrix} \mathbf{F}_t^{2G} \\ \mathbf{F}_r^{L8} \\ \mathbf{F}_r^{R8} \\ \mathbf{0}_{\bar{N}_s\times 1} \\ \mathbf{0}_{\bar{N}_b\times 1} \\ \mathbf{0}_{\bar{N}_p\times 1} \end{bmatrix} \quad \mathbf{F}_{RND}^9(t) = \begin{bmatrix} \mathbf{0}_{T_{dof}\times 1} \\ \mathbf{F}_r^{L9} \\ \mathbf{F}_r^{R9} \\ \mathbf{0}_{\bar{N}_s\times 1} \\ \mathbf{0}_{\bar{N}_b\times 1} \\ \mathbf{0}_{\bar{N}_p\times 1} \end{bmatrix} \quad \mathbf{F}_{RND}^{10}(t) = \begin{bmatrix} \mathbf{0}_{T_{dof}\times 1} \\ \mathbf{F}_r^{L10} \\ \mathbf{F}_r^{R10} \\ \mathbf{0}_{\bar{N}_s\times 1} \\ \mathbf{0}_{\bar{N}_b\times 1} \\ \mathbf{0}_{\bar{N}_p\times 1} \end{bmatrix} \quad \mathbf{F}_{RND}^{11}(t) = \begin{bmatrix} \mathbf{0}_{T_{dof}\times 1} \\ \mathbf{0}_{N_r\times 1} \\ \mathbf{0}_{N_r\times 1} \\ \mathbf{0}_{\bar{N}_s\times 1} \\ \mathbf{F}_b \\ \mathbf{F}_p \end{bmatrix}$$

Then, the load vector of the total train-slab track-bridge interaction system simultaneously excited by track irregularities and earthquakes $\mathbf{F}(t)$ can be expressed as

$$\mathbf{F}(t) = \begin{bmatrix} \mathbf{F}_t \\ \mathbf{F}_r^L \\ \mathbf{F}_r^R \\ \mathbf{F}_s \\ \mathbf{F}_b \\ \mathbf{F}_p \end{bmatrix} = \mathbf{F}_{GRT}(t) + \sum_{i=1}^{11} \mathbf{F}_{RND}^i(t) \tag{21}$$

4. Random vibration of train-slab track-bridge interaction system

Based on Eqs. (1) and (21), the three-dimensional equations of motion for a train-slab track-bridge interaction system can be expressed as

$$\mathbf{M}(t)\ddot{\mathbf{U}} + \mathbf{C}(t)\dot{\mathbf{U}} + \mathbf{K}(t)\mathbf{U} = \mathbf{F}(t) = \mathbf{F}_{GRT}(t) + \mathbf{F}_{RND}(t) \tag{22}$$

where $\mathbf{M}(t)$, $\mathbf{C}(t)$ and $\mathbf{K}(t)$ denote, respectively, the mass, damping and stiffness matrices of the total train-slab track-bridge interaction system; $\mathbf{U}$, $\dot{\mathbf{U}}$, and $\ddot{\mathbf{U}}$ denote, respectively, the displacement, velocity and acceleration vectors of the system; $\mathbf{F}(t)$ is the load vector of the system, which consists of two parts: the deterministic load $\mathbf{F}_{GRT}(t)$ induced by the gravity force of train and the random load $\mathbf{F}_{RND}(t)$ induced by track irregularities and earthquakes.

Thus the solution of Eq. (22) can be written as

$$\mathbf{U}(t) = \int_0^t \mathbf{H}(t,\tau)\mathbf{F}(\tau)d\tau \tag{23}$$

where $\mathbf{H}(t, \tau)$ is an impulse response matrix (Lu *et al*. 2009).

Appling the expectation operator $E[\cdot]$ to $\mathbf{U}(t)$, one obtains

$$\overline{\mathbf{U}}(t) = E[\mathbf{U}(t)] = \int_0^t \mathbf{H}(t,\tau)E[\mathbf{F}(\tau)]d\tau \tag{24}$$

where $\overline{\mathbf{U}}_{(t)}$ is the mean value (MV) vector of $\mathbf{U}(t)$

By assuming both the track irregularities and seismic accelerations to be zero-mean-valued random process, one obtains that $E[\mathbf{F}(\tau)]=\mathbf{F}_{GRT}(\tau)$, and meanwhile the covariance matrix $\mathbf{R}_{UU}(t)$ of the responses $\mathbf{U}(t)$ can be expressed as

$$\mathbf{R}_{UU}(t) = E[(\mathbf{U}-\mathbf{U})(\mathbf{U}-\mathbf{U})^{\mathbf{T}}] = \int_0^t \int_0^t \mathbf{H}(t,\tau_1)E[\mathbf{F}_{RND}(\tau_1)\mathbf{F}_{RND}^{\mathbf{T}}(\tau_2)]\mathbf{H}^{\mathbf{T}}(t,\tau_2)d\tau_1 d\tau_2 \tag{25}$$

where $E[\mathbf{F}_{RND}(\tau_1)\mathbf{F}_{RND}^{\mathbf{T}}(\tau_2)]$, denoting the covariance matrix of $\mathbf{F}_{RND}(t)$, can be written, according to the Wiener-Khintchine theorem, as

$$E[\mathbf{F}_{RND}(\tau_1)\mathbf{F}_{RND}^{\mathbf{T}}(\tau_2)] = \int_{-\infty}^{+\infty} \mathbf{S}_{FF}(\omega)e^{i\omega(\tau_1-\tau_2)}d\omega \tag{26}$$

where $\mathbf{S}_{FF}(\omega)$ is the PSD matrix of $\mathbf{F}_{RND}(t)$.

Substituting Eq. (26) into Eq. (25) and integrating with respect to τ over the frequency ω, one obtains

$$\mathbf{R}_{UU}(t) = \int_{-\infty}^{+\infty} \mathbf{S}_{UU}(\omega,t)d\omega \tag{27a}$$

$$\mathbf{S}_{UU}(\omega,t) = \int_0^t \int_0^t \mathbf{H}(t,\tau_1)\mathbf{S}_{FF}(\omega)\mathbf{H}^{\mathbf{T}}(t,\tau_2)d\tau_1 d\tau_2 \tag{27b}$$

where, obviously, $\mathbf{S}_{UU}(\omega, t)$ denotes the response PSD matrix.

5. Random vibration analysis of train-slab track-bridge interaction system by PEM

If the PSD function of $r(x)$ is $\mathbf{S}_{rr}(\Omega)$, the transformation $x = vt$ enables the PSD function of $r(t)$ to be expressed as

$$\mathbf{S}_{rr}(\omega) = \mathbf{S}_{rr}(\Omega)/v \qquad \omega = \Omega v$$

where ω (rad/s) is the time frequency, Ω (rad/m) is the spatial frequency, and v (m/s) is the train speed.

While, the PSD function of a_{gy} and a_{gz} are given as $S_{a_{gy}a_{gy}}(\omega)$ and $S_{a_{gz}a_{gz}}(\omega)$, respectively. As the duration of earthquakes is usually comparable with the time taken by the passage of a train over a bridge, it is reasonable to represent the earthquakes by the non-stationary random process as follow

$$a_{gy} = g(t)a_y \qquad a_{gz} = g(t)a_z$$

where $g(t)$ is a specified slowly varying modulation function, and a_y and a_z are the zero-mean-valued, stationary, seismic accelerations with PSDs of $S_{a_{gy}a_{gy}}(\omega)$ and $S_{a_{gz}a_{gz}}(\omega)$ respectively.

According to PEM and Eq. (21), the pseudo excitation $\tilde{\mathbf{F}}_{RND}(\omega,t)$ can be written as

$$\tilde{\mathbf{F}}_{RND}(\omega,t) = \sum_{i=1}^{11} \tilde{\mathbf{F}}_{RND}^i(\omega,t) \tag{28}$$

with

$$\tilde{\mathbf{F}}_{RND}^1(\omega,t) = \begin{bmatrix} \tilde{\mathbf{F}}_t^{1V}(\omega,t) \\ \tilde{\mathbf{F}}_r^{L1}(\omega,t) \\ \tilde{\mathbf{F}}_r^{R1}(\omega,t) \\ \mathbf{0}_{\overline{N}_s \times 1} \\ \mathbf{0}_{\overline{N}_b \times 1} \\ \mathbf{0}_{\overline{N}_p \times 1} \end{bmatrix} \quad \tilde{\mathbf{F}}_{RND}^2(\omega,t) = \begin{bmatrix} \tilde{\mathbf{F}}_t^{1C}(\omega,t) \\ \tilde{\mathbf{F}}_r^{L2}(\omega,t) \\ \tilde{\mathbf{F}}_r^{R2}(\omega,t) \\ \mathbf{0}_{\overline{N}_s \times 1} \\ \mathbf{0}_{\overline{N}_b \times 1} \\ \mathbf{0}_{\overline{N}_p \times 1} \end{bmatrix} \quad \tilde{\mathbf{F}}_{RND}^3(\omega,t) = \begin{bmatrix} \tilde{\mathbf{F}}_t^{1A}(\omega,t) \\ \tilde{\mathbf{F}}_r^{L3}(\omega,t) \\ \tilde{\mathbf{F}}_r^{R3}(\omega,t) \\ \mathbf{0}_{\overline{N}_s \times 1} \\ \mathbf{0}_{\overline{N}_b \times 1} \\ \mathbf{0}_{\overline{N}_p \times 1} \end{bmatrix} \quad \tilde{\mathbf{F}}_{RND}^4(\omega,t) = \begin{bmatrix} \mathbf{0}_{T_{dof} \times 1} \\ \tilde{\mathbf{F}}_r^{L4}(\omega,t) \\ \tilde{\mathbf{F}}_r^{R4}(\omega,t) \\ \mathbf{0}_{\overline{N}_s \times 1} \\ \mathbf{0}_{\overline{N}_b \times 1} \\ \mathbf{0}_{\overline{N}_p \times 1} \end{bmatrix}$$

$$\tilde{\mathbf{F}}_{RND}^5(\omega,t) = \begin{bmatrix} \tilde{\mathbf{F}}_t^{2V}(\omega,t) \\ \tilde{\mathbf{F}}_r^{L5}(\omega,t) \\ \tilde{\mathbf{F}}_r^{R5}(\omega,t) \\ \mathbf{0}_{\overline{N}_s \times 1} \\ \mathbf{0}_{\overline{N}_b \times 1} \\ \mathbf{0}_{\overline{N}_p \times 1} \end{bmatrix} \quad \tilde{\mathbf{F}}_{RND}^6(\omega,t) = \begin{bmatrix} \tilde{\mathbf{F}}_t^{2C}(\omega,t) \\ \tilde{\mathbf{F}}_r^{L6}(\omega,t) \\ \tilde{\mathbf{F}}_r^{R6}(\omega,t) \\ \mathbf{0}_{\overline{N}_s \times 1} \\ \mathbf{0}_{\overline{N}_b \times 1} \\ \mathbf{0}_{\overline{N}_p \times 1} \end{bmatrix} \quad \tilde{\mathbf{F}}_{RND}^7(\omega,t) = \begin{bmatrix} \tilde{\mathbf{F}}_t^{2A}(\omega,t) \\ \tilde{\mathbf{F}}_r^{L7}(\omega,t) \\ \tilde{\mathbf{F}}_r^{R7}(\omega,t) \\ \mathbf{0}_{\overline{N}_s \times 1} \\ \mathbf{0}_{\overline{N}_b \times 1} \\ \mathbf{0}_{\overline{N}_p \times 1} \end{bmatrix} \quad \tilde{\mathbf{F}}_{RND}^8(\omega,t) = \begin{bmatrix} \tilde{\mathbf{F}}_t^{2G}(\omega,t) \\ \tilde{\mathbf{F}}_r^{L8}(\omega,t) \\ \tilde{\mathbf{F}}_r^{R8}(\omega,t) \\ \mathbf{0}_{\overline{N}_s \times 1} \\ \mathbf{0}_{\overline{N}_b \times 1} \\ \mathbf{0}_{\overline{N}_p \times 1} \end{bmatrix}$$

$$\tilde{\mathbf{F}}_{RND}^9(\omega,t) = \begin{bmatrix} \mathbf{0}_{T_{dof} \times 1} \\ \tilde{\mathbf{F}}_r^{L9}(\omega,t) \\ \tilde{\mathbf{F}}_r^{R9}(\omega,t) \\ \mathbf{0}_{\overline{N}_s \times 1} \\ \mathbf{0}_{\overline{N}_b \times 1} \\ \mathbf{0}_{\overline{N}_p \times 1} \end{bmatrix} \quad \tilde{\mathbf{F}}_{RND}^{10}(\omega,t) = \begin{bmatrix} \mathbf{0}_{T_{dof} \times 1} \\ \tilde{\mathbf{F}}_r^{L10}(\omega,t) \\ \tilde{\mathbf{F}}_r^{R10}(\omega,t) \\ \mathbf{0}_{\overline{N}_s \times 1} \\ \mathbf{0}_{\overline{N}_b \times 1} \\ \mathbf{0}_{\overline{N}_p \times 1} \end{bmatrix} \quad \tilde{\mathbf{F}}_{RND}^{11}(\omega,t) = \begin{bmatrix} \mathbf{0}_{T_{dof} \times 1} \\ \mathbf{0}_{N_r \times 1} \\ \mathbf{0}_{N_r \times 1} \\ \mathbf{0}_{\overline{N}_s \times 1} \\ \tilde{\mathbf{F}}_b(\omega,t) \\ \tilde{\mathbf{F}}_p(\omega,t) \end{bmatrix}$$

Thus, the pseudo response caused by $\tilde{\mathbf{F}}_{RND}(\omega,t)$ is

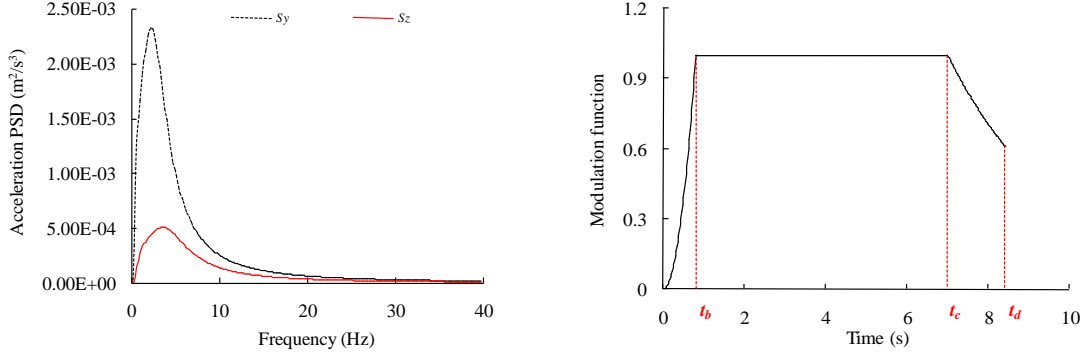$$\tilde{\mathbf{U}}(\omega,t) = \int_0^t \mathbf{H}(t,\tau)\tilde{\mathbf{F}}_{RND}(\tau)d\tau \tag{29}$$

According to Eq. (27b)

$$\mathbf{S}_{UU}(\omega,t) = \tilde{\mathbf{U}}^*(\omega,t)\tilde{\mathbf{U}}^{\mathbf{T}}(\omega,t)$$

where the superscript '*' denotes complex conjugate.

6. Solution procedure

The solution procedures for efficiently evaluating the random vibration analysis of train-slab track-bridge system are as follows

(a) PSDs of lateral and vertical seismic acceleration   (b) Modulation function $g(t)$

Fig. 2 Plots of earthquake used in the numerical example for DBGA = 0.15 g

(a) Calculate the MV of the dynamic responses according to Eq. (24).

(b) Select the jth discrete frequency ω_j (j=1, 2, 3,…, m), where m denotes the total number of discrete frequencies considered.

(c) Constitute the pseudo excitation $\tilde{\mathbf{F}}_{RND}(\omega,t)$ for each selected frequency of track irregularities and seismic accelerations according to Eq. (28).

(d) Solve pseudo response $\tilde{\mathbf{U}}(\omega_j,t)$ according to Eq. (29) by step-by-step integration method.

(f) Compute the PSD $\mathbf{S}_{U_{out}}(\omega_j,t)$ of responses of interest and the corresponding standard deviation (SD) $\sigma_{U_{out}}(t)$, according to

$$\mathbf{S}_{Uout}(\omega_j,t) = \tilde{\mathbf{U}}_{out}(\omega_j,t)\tilde{\mathbf{U}}^*_{out}(\omega_j,t) \qquad \sigma^2_{U_{out}}(t) = \sum_{j=1}^{m}\mathbf{S}_{U_{out}}(\omega_j,t)\Delta\omega$$

(g) Estimate the global maximum value max($\mathbf{U}_{out}(t)$) and minimum value min($\mathbf{U}_{out}(t)$) of responses by first-passage failure criterion, if necessary

$$\text{max}(\mathbf{U}_{out}(t)) = \text{max}(\text{MV}(t)) + (E(\bar{\eta}_{\mathbf{U}_{out}}) + \kappa\sigma_{\bar{\eta}})\bar{\sigma}_{\mathbf{U}_{out}} \tag{30a}$$

$$\text{min}(\mathbf{U}_{out}(t)) = \text{min}(\text{MV}(t)) - (E(\bar{\eta}_{\mathbf{U}_{out}}) + \kappa\sigma_{\bar{\eta}})\bar{\sigma}_{\mathbf{U}_{out}} \tag{30b}$$

7. Illustrative examples

7.1 Properties of train-slab track-bridge interaction system

A fifteen-span simply supported girder high-speed railway bridge, with the span length of 32 m and the pier height of 22 m, is considered as shown in Fig. 1. The central part of railway slab track is supported on bridge, while the left and right parts of the track are supported on subgrades adjacent to bridge. The lengths of element of rail, slab and bridge girder are all equal to fastener spacing of 0.625 m, while the length of pier element equals 1.0 m. An ICE3 high-speed train (Du *et al*. 2012) comprises front and rear motor cars and six identical trailer cars moving at constant

Table 1 Fundamental properties of trailer car and motor car

Notation	Unit	Value	Notation	Unit	Value
m_c / m_{Jc}	kg	$4.40\times10^4 / 4.80\times10^4$	k_{pz} / k_{Jpz}	N/m	$0.70\times10^6 / 1.00\times10^6$
m_t / m_{Jt}	kg	$2.40\times10^3 / 3.20\times10^3$	c_{sy} / c_{Jsy}	N·s/m	$2.50\times10^4 / 3.00\times10^4$
m_w / m_{Jw}	kg	$2.40\times10^3 / 2.40\times10^3$	c_{sz} / c_{Jsz}	N·s/m	$5.00\times10^4 / 4.00\times10^4$
W_{axle} / W_{Jaxle}	kg	$1.46\times10^4 / 1.60\times10^4$	c_{py} / c_{Jpy}	N·s/m	0.00 / 0.00
I_{cx} / I_{Jcx}	kg·m²	$1.00\times10^5 / 1.15\times10^5$	c_{pz} / c_{Jpz}	N·s/m	$4.00\times10^4 / 3.00\times10^4$
I_{cy} / I_{Jcy}	kg·m²	$2.70\times10^5 / 2.70\times10^5$	L_c / L_{Jc}	m	8.6875 / 8.6875
I_{cz} / I_{Jcz}	kg·m²	$2.70\times10^5 / 2.70\times10^5$	L_t / L_{Jt}	m	1.25 / 1.25
I_{tx} / I_{Jtx}	kg·m²	$1.80\times10^3 / 3.20\times10^3$	b_0 / b_{J0}	m	0.748 / 0.748
I_{ty} / I_{Jty}	kg·m²	$2.20\times10^3 / 7.20\times10^3$	b_1 / b_{J1}	m	0.95 / 0.95
I_{tz} / I_{Jtz}	kg·m²	$2.20\times10^3 / 6.80\times10^3$	b_2 / b_{J2}	m	1.00 / 1.00
I_{tx} / I_{Jtx}	kg·m²	$1.10\times10^3 / 1.20\times10^3$	b_3 / b_{J3}	m	0.95 / 0.95
I_{tz} / I_{Jtz}	kg·m²	$1.10\times10^3 / 1.20\times10^3$	b_4 / b_{J4}	m	1.00 / 1.00
k_{sy} / k_{Jsy}	N/m	$2.80\times10^5 / 2.40\times10^5$	h_1 / h_{J1}	m	1.14 / 1.00
k_{sz} / k_{Jsz}	N/m	$3.00\times10^5 / 4.00\times10^5$	h_2 / h_{J2}	m	-0.14 / 0.10
k_{py} / k_{Jpy}	N/m	$5.00\times10^6 / 3.00\times10^6$	h_3 / h_{J3}	m	0.24 / 0.14

Table 2 Fundamental properties of slab track and bridge

Notation	Item	Unit	Value
Slab track			
E_r	Young's modulus of rail	N/m²	2.06×10^{11}
I_{ry}	Flexural moment of inertia about y axis of cross section of rail	m⁴	3.217×10^{-5}
I_{rz}	Flexural moment of inertia about z axis of cross section of rail	m⁴	5.24×10^{-6}
$\bar{m}_r$	Mass per unit length of rail	kg/m	60.64
E_s	Young's modulus of slab	N/m²	3.6×10^{10}
I_{sy}	Flexural moment of inertia of cross section of slab	m⁴	1.4×10^{-3}
I_{sz}	Flexural moment of inertia of cross section of slab	m⁴	0.219
$\bar{m}_s$	Mass per unit length of slab	kg/m	1.2×10^3
k_{rsy}	Lateral stiffness of fastener	N/m	3.0×10^7
k_{rsz}	Vertical stiffness of fastener	N/m	5.0×10^7
c_{rsy}	Lateral damping coefficient of fastener	N·s/m	5.0×10^4
c_{rsz}	Vertical damping coefficient of fastener	N·s/m	6.0×10^4
$\bar{k}_{sby}$	Lateral stiffness of CA layer per unit length	N/m²	1.5×10^9
$\bar{k}_{sbz}$	Vertical stiffness of CA layer per unit length	N/m²	1.5×10^9
Bridge girder			
E_b	Young's modulus of girder	N/m²	3.45×10^{10}
I_{by}	Flexural moment of inertia about y axis of cross section of girder	m⁴	12.744
I_{bz}	Flexural moment of inertia about z axis of cross section of girder	m⁴	96.435
$\bar{m}_b$	Mass per unit length of girder	kg/m	2.972×10^4
ω_{b1}	The fundamental frequency of girder	Hz	5.58
ω_{b2}	The second natural frequency of girder	Hz	13.26
k_{bby}	Lateral spring stiffness of bearing	N/m	6.0×10^8
k_{bbz}	Vertical spring stiffness of bearing	N/m	6.0×10^9
Bridge pier			
E_p	Young's modulus of pier	N/m²	3.45×10^{10}
I_{px}	Flexural moment of inertia about x axis of cross section of pier	m⁴	73.23
$\bar{m}_p$	Mass per unit length of pier	kg/m	5.2×10^4

velocity v. The fundamental properties of the vehicle, track and bridge are listed in Tables 1 and 2. The German high-speed track irregularity PSD functions (Zhai and Cai 2002) are adopted. The seismic acceleration PSDs of the Clough-Penzien model (Clough and Penzien 1993) and the uniform modulation function $g(t)$ are shown in Fig. 2. Herein DBGA means the design basic acceleration of ground motion, t_b and t_c the instants at the start and end of the stationary main shock respectively, and t_d the duration of earthquakes. It is assumed that the DBGA=0.15 g, t_b=0.8 s, t_c=7.0 s and t_d=8.41 s. In addition, the spatial frequency of the PSDs of track irregularity range from $0.004 \times 2\pi$ to $1 \times 2\pi$ rad/m, while the frequency of the PSDs of seismic acceleration lie in the range of 0~40 Hz.

7.2 Comparison PEM with MCM

The maximum dynamic responses of train-track/bridge subjected to earthquake excitations are usually of most interest for us. A conventional method of estimation is to pick the maximum values from a set of response samples. The sample size must be large enough to ensure the reliability of the estimation because of the random nature of track irregularities and earthquakes, which may lead to intolerable computer time. However, based on PEM, the global upper and lower boundary of non-stationary random responses can be evaluated efficiently and accurately according to Eq. (30) in which κ=3 is adopted to ensure the probability is higher than 98% (Zhang *et al*. 2010a).

For the purpose of comparison, the random responses of the train-slab track-bridge interaction system calculated by PEM are compared with those by MCM with 1500 samples of track irregularities and seismic accelerations. Herein the method proposed by Chen and Zhai (1999) is implemented to generate the track irregularities sample $r(x)$ from the PSD function. The train is assumed to pass through the bridge with a constant speed 83.33 m/s (300 km/h). Figs. 3-5 show the estimated upper and lower boundary of the responses by PEM and the corresponding extreme values of each time-domain responses by MCM. In Fig. 4(a), the minus sign '-' means that dynamic vertical wheel/rail force is bigger than the static wheel load. The variation ratio VR_1 of the responses of train, bridge girder and pier, determined according to Eq. (31), is shown in Table 3.

$$VR_1 = \frac{\max\left|R_{MCM}^E(i)\right| - \min\left|R_{MCM}^E(i)\right|}{\min\left|R_{MCM}^E(i)\right|} \times 100\% \quad (i = 1 \sim 1500) \tag{31}$$

where R_{MCM}^E denote the extreme values of each time-domain response obtained by MCM, and i the sample size of track irregularities and seismic accelerations.

In the following examples, 'motor car' and 'trailer car' considered mean, respectively, the rear motor car, and 1st trailer car connecting with the rear motor car (see Fig. 1); 'midpoint', 'endpoint' and 'pier top' are, respectively, the midpoint, the right endpoint and the top of the right pier of the eighth span for the fifteen-span bridge; 'wheel/rail force' is the contact force between the 2nd wheelset of rear motor car or of 1st trailer car and left rail.

From Table 3 and Figs. 3-5, the following observations can be made easily: (1) There exist dramatic variations for the extreme values of almost each of time-domain responses by MCM. For example, the variation ratio VR_1 of lateral acceleration of trailer carbody, lateral wheel/rail force of trailer car, wheel load decrement ratio of trailer car and lateral acceleration of bridge girder midpoint among the 1500 samples, approach 190.2%, 125.6%, 88.9%, and 73.4%, respectively. Furthermore, larger sample size of track irregularities and seismic accelerations tends to enlarge
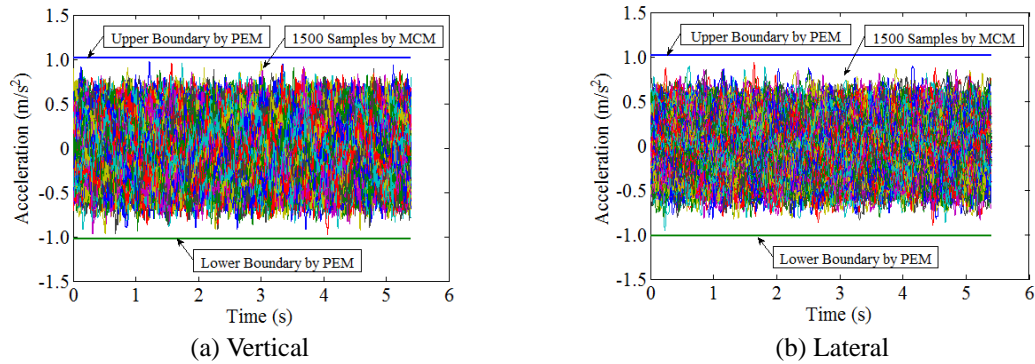
(a) Vertical (b) Lateral

Fig. 3 Comparison of trailer carbody acceleration

(a) Wheel load decrement ratio (b) Lateral wheel/rail force
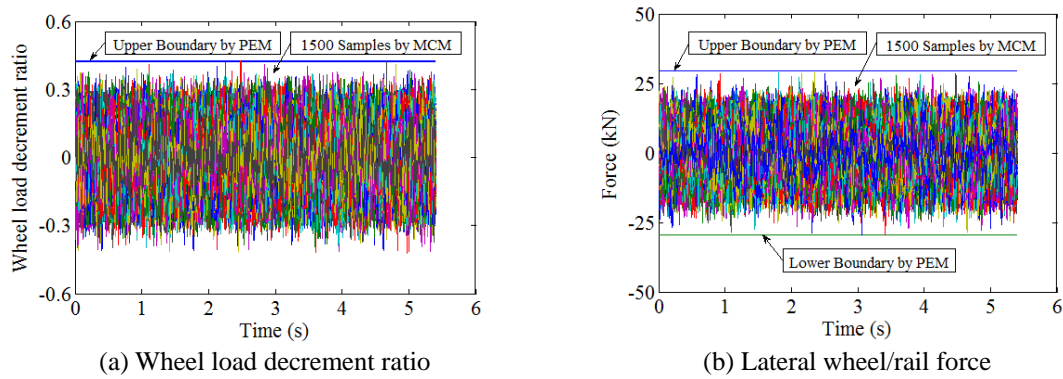
Fig. 4 Comparison of wheel/rail interaction for motor car
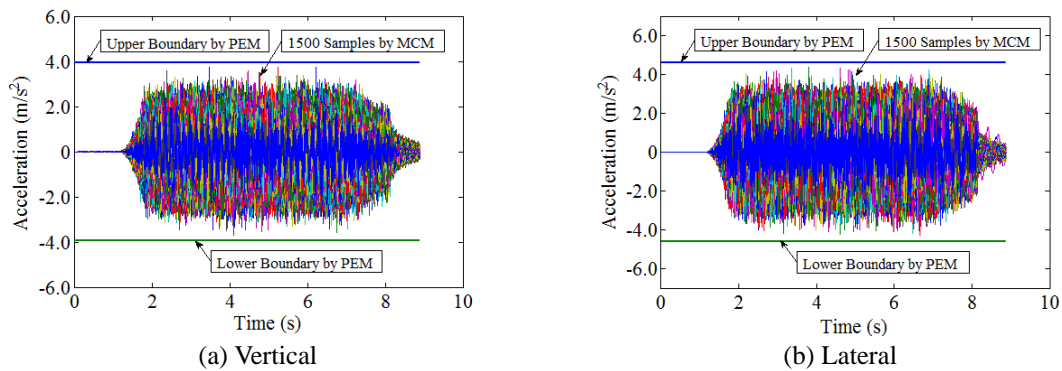

(a) Vertical (b) Lateral

Fig. 5 Comparison of acceleration of bridge girder midpoint

the variation ratio VR_1. (2) All of extreme values of responses obtained by MCM fall with the corresponding limits of upper and lower boundary by PEM. (3) Compared with MCM, PEM helps to save computer time drastically. For example, the total CPU times for PEM with 200 discrete frequencies and for MCM with only 100 samples are 12.4 hours and 116.4 hours, respectively, on a 3.4 GHz personal computer. The latter equals about 9.4 times the former. As shown Table 3, the

Table 3 Variation ratio VR_1 of the responses (%) and CPU times (h)

Item		The sample size of track irregularities and seismic accelerations					
		50	100	300	500	1000	1500
Vertical acceleration of carbody	Motor car	64.9	88.2	117.5	153.2	153.2	153.2
	Trailer car	93.8	93.8	121.1	130.8	141.1	141.1
Lateral acceleration of carbody	Motor car	116.4	158.1	161.9	161.9	193.8	193.8
	Trailer car	131.6	131.6	163.7	163.7	183.6	190.2
Vertical acceleration of rear bogie	Motor car	45.5	50.5	63.5	75.0	79.4	82.9
	Trailer car	38.0	44.9	63.5	72.3	85.9	86.7
Lateral acceleration of rear bogie	Motor car	55.0	78.1	100.3	100.3	129.9	136.8
	Trailer car	68.1	71.9	93.8	93.8	128.0	128.0
Lateral wheel/rail force	Motor car	68.7	68.7	116.9	116.9	122.8	122.8
	Trailer car	64.4	71.5	101.4	110.9	125.6	125.6
Wheel load decrement ratio	Motor car	51.2	69.4	84.3	87.1	89.9	89.9
	Trailer car	50.4	60.9	74.5	81.5	81.5	88.9
Vertical acceleration of bridge girder midpoint		55.7	61.5	71.3	71.3	83.8	83.8
Lateral acceleration of bridge girder midpoint		49.4	54.8	65.2	69.4	73.4	73.4
Lateral acceleration of bridge girder endpoint		51.0	54.4	59.3	65.4	77.5	77.5
CPU times		58.2	116.4	349.1	581.8	1163.6	1745.4

computer time of MCM is barely tolerable in investigating the random vibration of train-slab track-bridge interaction system.

7.3 Analysis of the PSD characteristic of the random vibration responses of bridge and train

The random vibration responses of bridge and train calculated by PEM with train speed of 300 km/h are still used.

The PSDs of vertical and lateral acceleration of bridge girder midpoint to the passage of the train shaken by track irregularities and earthquakes are plotted in Fig. 6. It can be seen from Fig. 6(a) that there exists only one dominant vibration frequency (DVF) of 5.34 Hz, which is very close to the vertical fundamental frequency of bridge girder of 5.58 Hz. Similarly, only one DVF of 3.07 Hz can be found from Fig. 6(b), which means the lateral fundamental frequency of the total bridge (including girder and pier) is about 3.0 Hz.

Fig. 7 exhibit the PSDs of vertical and lateral accelerations of trailer carbody. As can be seen, the PSDs change violently with vibration frequency, implying the great influence of track irregularities and earthquakes on the dynamic response of carbody. Of interest is that there exist two DVFs with DVF1 = 0.83 Hz and DVF2 = 5.19 Hz in Fig. 7(a), which are approximately equal to the vertical fundamental frequency of trailer carbody and of bridge girder, respectively. Similarly, two DVFs with DVF1 = 1.49 Hz and DVF2 = 2.98 Hz can be seen easily from Fig. 7(b), which are also close to the lateral fundamental frequency of trailer carbody and of the total bridge, respectively. Obviously, the vertical DVF1 and the lateral DVF1 are mainly excited by track irregularities, and vertical DVF2 and the lateral DVF2 are mainly induced by bridge vibration under the shake of earthquakes. On the other hand, the vertical and lateral PSDs excited by track

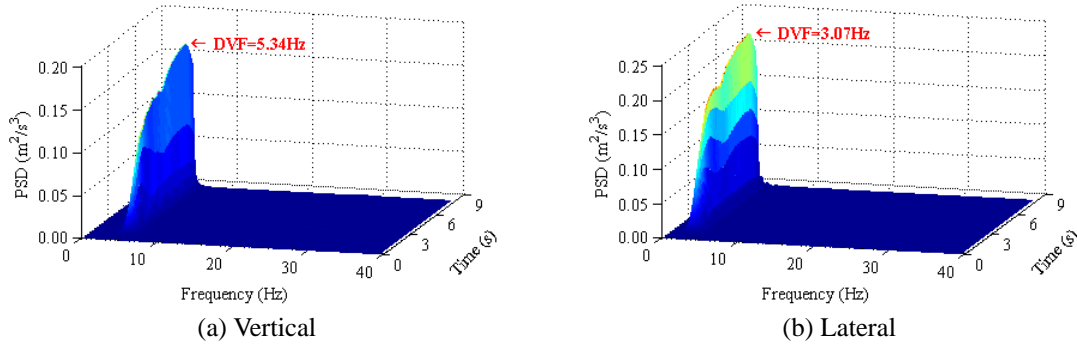(a) Vertical   (b) Lateral

Fig. 6 PSD of acceleration of bridge girder midpoint

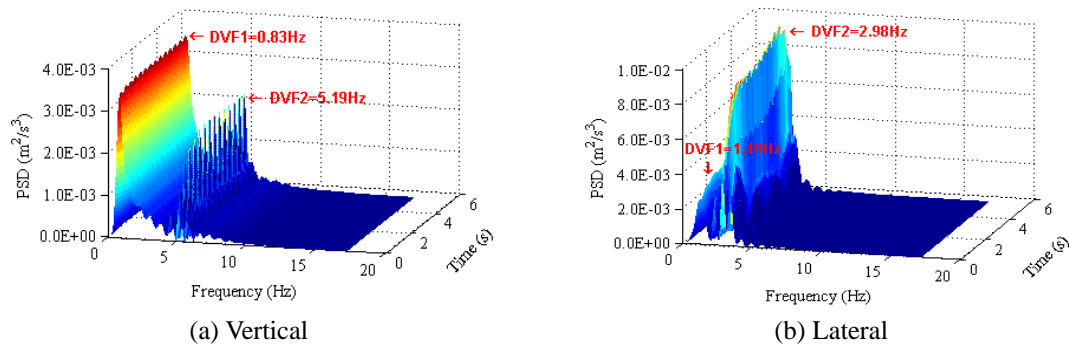

(a) Vertical   (b) Lateral

Fig. 7 PSD of acceleration of trailer carbody

irregularities vary only slightly with time, which indicates the influence of bridge vibration on carbody vibration is insignificant if there is no earthquake because of the comparatively high mass and flexural rigidity of bridge. However, the vertical PSD induced by earthquakes vary periodically with the vehicle passing different bridge girder (see Fig. 7(a)), while the similar trend can't be found for the lateral PSD induced by earthquakes (see Fig. 7(b)).

The similar phenomenon for vertical and lateral accelerations of motor carbody can be also observed. Herein it is not discussed in detail to save the length of the paper.

7.4 Influence of train speed on the random vibration characteristic of bridge and train

In reality, the train may move over the bridge at various speed during earthquakes. There exists a need to investigate the random vibration characteristic of train moving over bridge under various train speed, as they may be different. The train is assumed to move over the bridge with speed varying from 150 to 410 km/h at 20 km/h intervals. The other parameters are the same as listed in subsection 7.1. The maximal values of PSD and the DVF of bridge and train with respect to train speed are plotted in Figs. 8-12.

A conclusion can be drawn from Fig. 8 that both the maximal values of PSD and the DVF of bridge vary little no matter how changes the train speed, which indicates that the vertical and lateral vibration of bridge are induced basically by earthquakes rather than by the train and track irregularities.
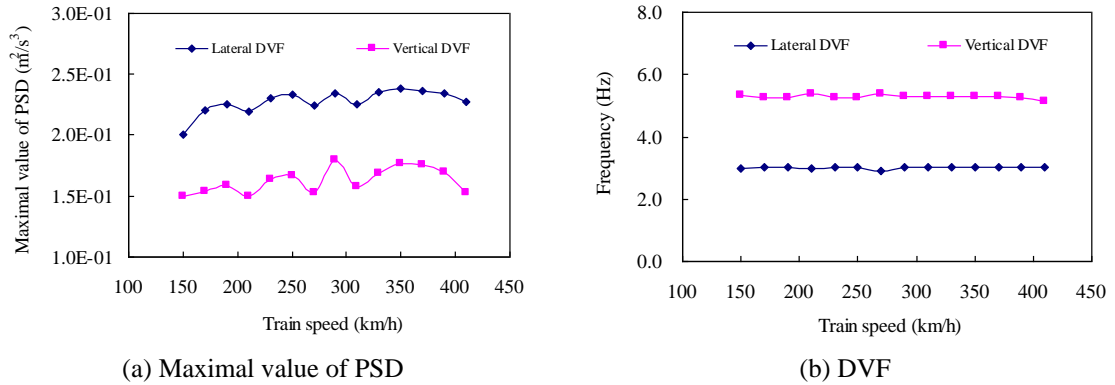
(a) Maximal value of PSD   (b) DVF

Fig. 8 Bridge girder midpoint acceleration with respect to train speed

(a) Maximal value of PSD   (b) DVF
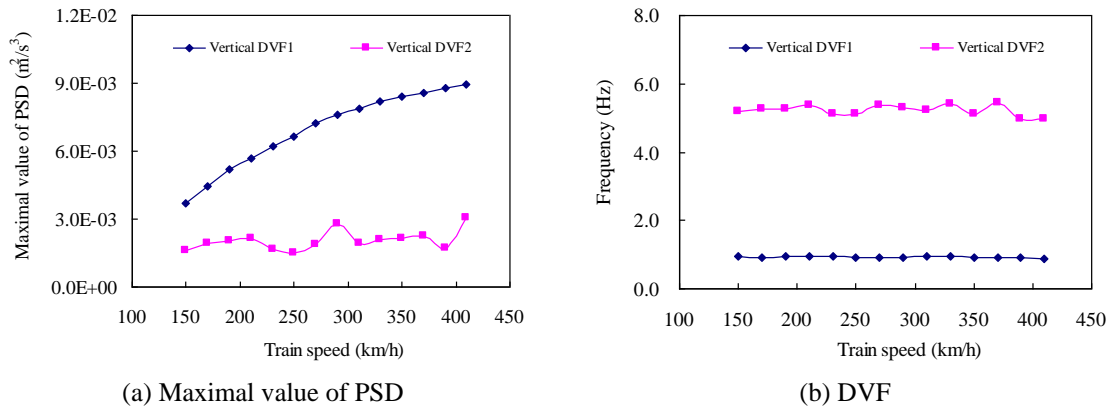
Fig. 9 Motor carbody vertical acceleration with respect to train speed
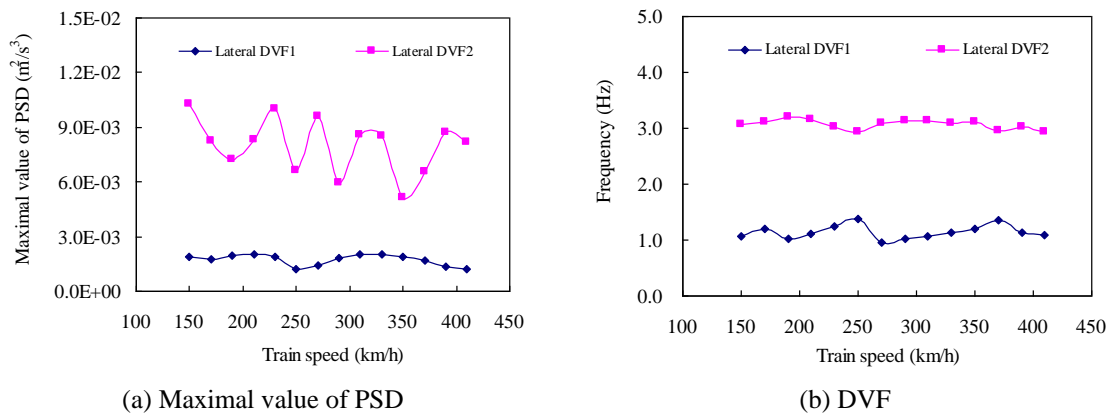

(a) Maximal value of PSD   (b) DVF

Fig. 10 Motor carbody lateral acceleration with respect to train speed

From Figs. 9-12, the following observations can be made easily: (1) The DVF1 and DVF2 for both vertical and lateral accelerations of carbody change slightly around the corresponding fundamental

frequencies of train and bridge with the rising of train speed (see Figs. 9(b), 10(b), 11(b) and 12(b)). (2) For carbody vertical acceleration, the maximal values of PSD of DVF1 increase as the train speed increases (see Figs. 9(a) and 11(a)). (3) The maximal values of PSD of DVF1 for carbody lateral acceleration don't show a trend of monotonic increase for higher train speed (see Figs. 10(a) and 12(a)). This trend can be also found from the maximal values of PSD of DVF2 for both vertical and lateral accelerations of carbody (see Figs. 9(a), 10(a), 11(a) and 12(a)). (4) For carbody vertical vibration, the maximal values of PSD of DVF1 are generally bigger than those of DVF2 (see Figs. 9(a) and 11(a)), implying that the influence of track irregularities is more obvious than that of earthquakes. However the opposite is the case for carbody lateral vibration (see Figs. 10(a) and 12(a)).

7.5 Random vibration characteristic of train and bridge under track irregularities

To investigate the random vibration characteristic of the train-slab track-bridge interaction system under track irregularities, four running cases with train speeds of v=55.56 m/s (200 km/h),
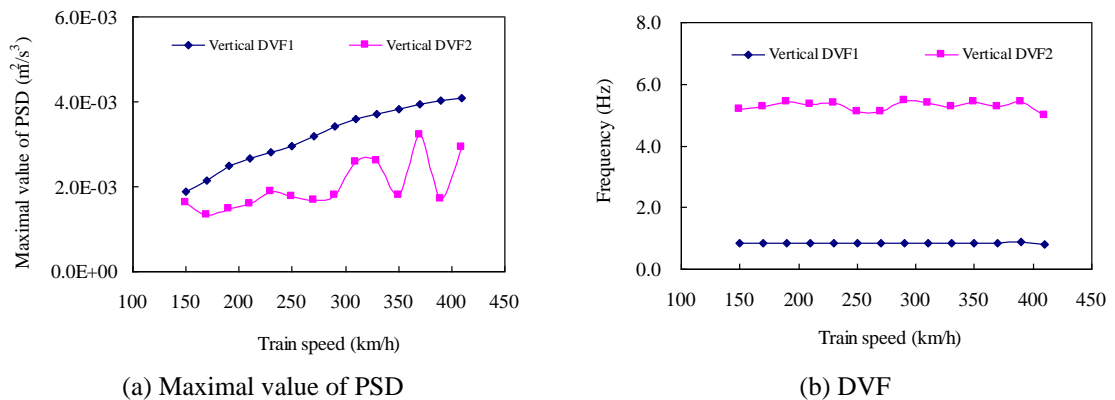

(a) Maximal value of PSD   (b) DVF

Fig. 11 Trailer carbody vertical acceleration with respect to train speed
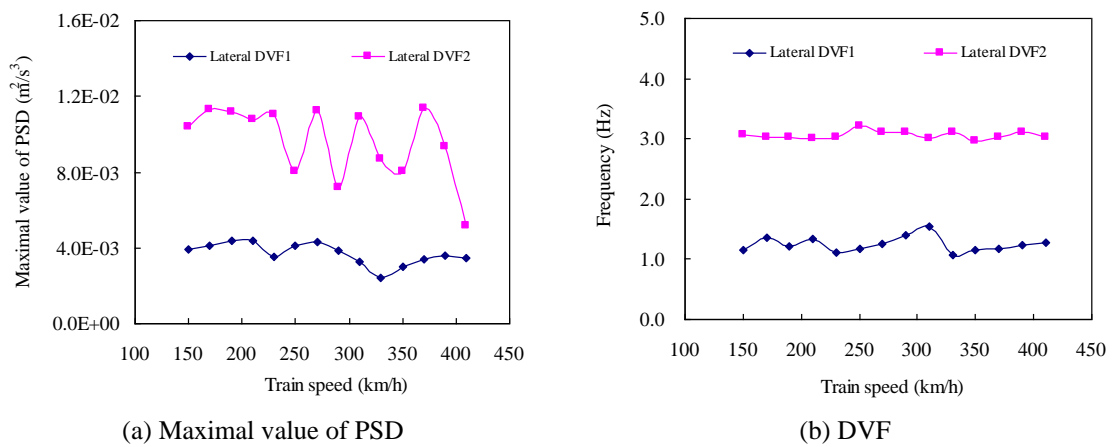

(a) Maximal value of PSD   (b) DVF

Fig. 12 Trailer carbody lateral acceleration with respect to train speed

Table 4 DVFs of the random responses (Hz)

Item		Train speed (m/s)			
		55.56	69.44	83.33	97.22
Vertical acceleration of carbody	Motor car	0.82	0.82	0.86	0.86
	Trailer car	0.74	0.77	0.77	0.77
Lateral acceleration of carbody	Motor car	1.06	1.10	1.06	1.07
	Trailer car	1.06	1.10	1.14	1.07
Pitching acceleration of carbody	Motor car	1.06	1.06	1.10	1.07
	Trailer car	0.98	1.03	1.06	1.07
Yawing acceleration of carbody	Motor car	1.22	1.14	1.19	1.11
	Trailer car	1.27	1.27	1.32	1.34
Vertical acceleration of rear bogie	Motor car	4.69, 21.4, 44.7	6.08, 27.0, 55.8	6.09, 32.4, 67.0	6.37, 39.2, 78.2
	Trailer car	4.87, 21.4, 44.7	6.54, 28.0, 55.8	7.85, 33.6, 67.0	8.22, 39.2, 78.2
Lateral acceleration of rear bogie	Motor car	5.83	8.44	9.42	10.2
	Trailer car	5.84, 17.4	6.78, 18.8	8.14, 21.7	10.2
Pitching acceleration of rear bogie	Motor car	5.83	6.31	6.55, 50.1, 83.3	6.60, 58.4, 97.2
	Trailer car	11.6, 33.4, 55.5	14.0, 41.7, 69.4	16.8, 50.1, 83.3	19.0, 58.4, 97.2
Yawing acceleration of rear bogie	Motor car	14.5	14.6	14.6	14.7
	Trailer car	32.2	32.4	32.4	32.7
Lateral acceleration of wheelset	Motor car	10.4, 15.6	11.3, 15.7	12.1, 16.2	12.3, 16.4
	Trailer car	13.0, 24.1, 33.2	14.0, 26.0	15.7	16.4, 32.7
Wheelset lateral force	Motor car	1.02, 15.6	1.03, 12.6, 15.7	1.00, 16.2	1.00, 15.8
	Trailer car	1.27, 14.0, 33.4	1.23, 5.87, 16.8	1.27, 6.31, 16.8	1.24, 18.3, 33.7
Vertical acceleration of bridge girder midpoint		5~7, 22~25, 35~43	4~6, 25~33, 51~57	5~8, 30~40, 62~69	4~7, 35~43, 72~81

69.44 m/s (250 km/h), 83.33 m/s (300 km/h) and 97.22 m/s (350 km/h) are considered. The DVFs of the train and bridge obtained by PEM are shown in Table 4 and Figs. 13-16. Some conclusions can be drawn from Table 4 and Figs. 13-16: (1) The DVFs of vertical, lateral, pitching, and yawing accelerations of carbody are approximately equal to the corresponding fundamental frequencies of carbody no matter how train speed changes. (2) There exist three DVFs for the vertical acceleration of bogie, e.g., 6.09 (motor car) or 7.85 (trailer car), 33 and 67 Hz for v=83.33 m/s. It is found that the vertical vibration frequency f_t of bogie, the half of bogie axle base L_t, and the train speed v satisfy the relation: $f_t=v/(n{\times}L_t)$, n=1, 2, 3, …, ∞, where relatively large contributions are made by harmonic components with n=1, 2 (see Fig. 14(a)). (3) In general, there also exist three DVFs for the pitching acceleration of bogie. Of interesting is that the pitching vibration frequency f_t of bogie, the half of bogie axle base L_t, and the train speed v satisfy the relation: $f_t=n{\cdot}v/(4{\times}L_t)$, n=1, 3, and 5. Furthermore, the contributions of DVF2 and DVF3 show a trend of increase for higher train speeds (see Fig. 15). (4) Compared the lateral vibration of wheelset with the yawing vibration of bogie, one can find the latter may have significant influence on the former at certain train speeds. (5) the DVFs of wheelset lateral force are very coincident with those of carbody yawing acceleration, bogie yawing acceleration, and wheelset lateral acceleration. (6) Similar with the cases of bogie vertical and pitching accelerations, the vertical acceleration of bridge girder
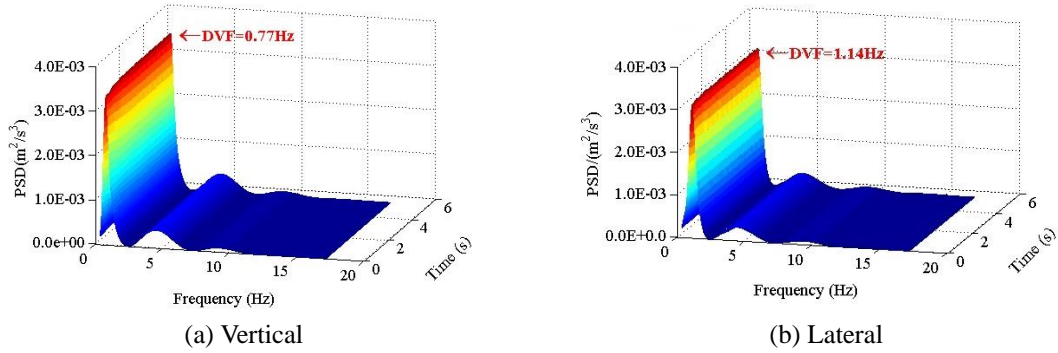
(a) Vertical   (b) Lateral

Fig. 13 PSD of acceleration of trailer carbody (v=83.33 m/s)

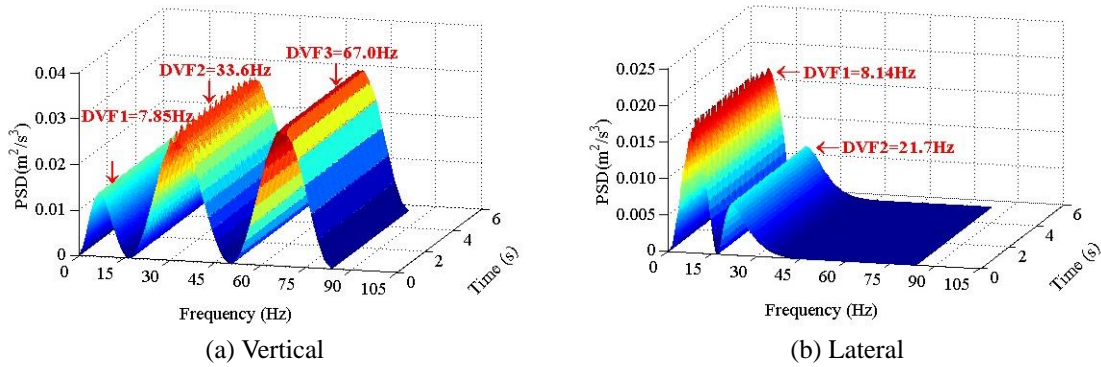(a) Vertical   (b) Lateral

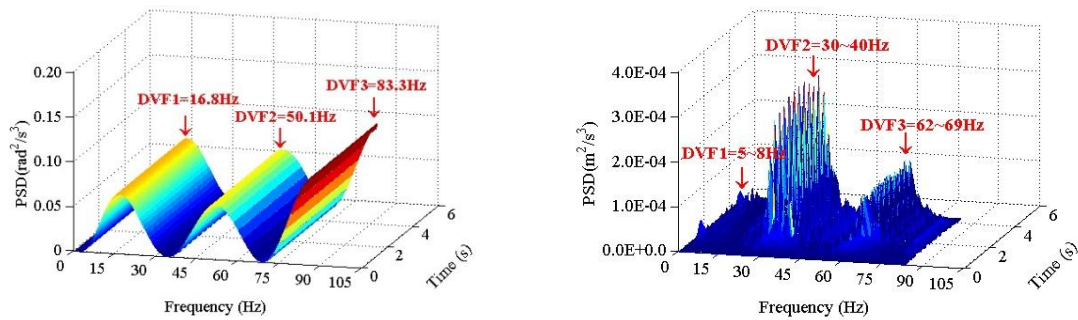Fig. 14 PSD of acceleration of rear bogie of trailer car (v=83.33 m/s)

Fig. 15 PSD of pitching acceleration of rear bogie of trailer car (v=83.33 m/s)

Fig. 16 PSD of vertical acceleration of bridge girder midpoint (v=83.33 m/s)

midpoint have three DVFs of 5~7, 22~25, and 35~43 Hz for v=55.56 m/s, 4~6, 25~33, and 51~57 Hz for v=69.44 m/s, 5~8, 30~40, and 62~69 Hz for v=83.33 m/s and 4~7, 35~43, and 72~81 Hz for v=97.22 m/s. Obviously, the DVF1 vary slightly around the fundamental frequency of the girder ω_{b1}=5.58 Hz under various train speeds. However, both the DVF2 and DVF3 increase as the train speed increases, whose trends quite coincide with those of bogie vertical acceleration (see Figs. 14(a) and 16). (7) The peak values of the vertical and lateral acceleration PSD of trailer

carbody in Fig. 7 are 3.76×10^{-3} and 8.63×10^{-3} m^2/s^3, respectively, while those in Fig. 13 are 3.65×10^{-3} and 3.17×10^{-3} m^2/s^3, respectively, which indicates that the effect of earthquakes on carbody lateral vibration of carbody is greater than that on the vertical vibration of carbody. The peak values of the vertical acceleration PSD of bridge girder midpoint in Figs. 6(a) and 16 are 0.172 and 3.34×10^{-4} m^2/s^3, respectively. The latter is quite smaller than the former, indicating that the effect of track irregularities and moving train can be neglected when computing the response of bridge to earthquakes. Similarly, one can also obtain that the effect of track irregularities and moving train on the lateral vibration of bridge is significantly smaller than that of earthquakes.

8. Conclusions

In this study, the three-dimensional vibration model of train-slab track-bridge interaction system is firstly established by FEM, the equations of motion for the entire system are then derived by means of energy principle. The excitations caused by random track irregularities and seismic accelerations are transformed into a series of deterministic pseudo-harmonic excitation vectors via PEM. Taking a fifteen-span simply supported girder bridge as an example, the random vibration characteristic of the coupled system are investigated. From the numerical results obtained in this work, the following conclusions can be drawn:

• Compared with MCM, PEM can not only save computer time dramatically but also ensure computational accuracy in evaluating the possible extreme values of the random vibration responses of the train-track-bridge interaction system simultaneously excited by track irregularities and earthquakes.

• The DVFs of both vehicle and bridge are always very close to their respective fundamental frequencies no matter train speed is moderate or high under the action of earthquakes.

• It is the earthquakes rather than the train and track irregularities that induces basically the vertical and lateral vibration of bridge.

• Unlike the case of carbody vertical vibration, the maximal values of PSD induced by track irregularities for carbody lateral acceleration don't show a trend of monotonic increase as the rising of train speed, and the influence of earthquakes on carbody lateral vibration is more visible than that of track irregularities.

• The DVFs of train-slab track-bridge interaction system under the action of track irregularities can be observed clearly from the time-dependent PSDs obtained by PEM, which may provide a powerful guidance in the design of the dynamic parameters of train, track and bridge as well as in the maintenance of railway lines.

Acknowledgements

References

Antolín, P., Zhang, N., M. Goicolea, J., Xia, H., Á. Astiz, M. and Oliva, J. (2013), "Consideration of nonlinear wheel-rail contact forces for dynamic vehicle-bridge interaction in high-speed railways", *J. Sound Vib.*, **332**(5), 1231-1251.

Chen, G. and Zhai, W.M. (1999), "Numerical simulation of the stochastic process of railway track irregularities", *J. Southwest Jiaotong Univ.*, **34**(2), 138-142.

Clough, R.W. and Penzien, J. (1993), *Dynamics of structures*, McGraw-Hill, New York, USA.

Du, X.T., Xu, Y.L. and Xia, H. (2012), "Dynamic interaction of bridge-train system under non-uniform seismic ground motion", *Earthq. Engng. Struct. Dyn.*, **41**(1) 139-157.

Frýba, L. and Yau, J.D. (2009), "Suspended bridges subjected to moving loads and support motions due to earthquake", *J. Sound Vib.*, **319**(1-2), 218-227.

Gao, L., Yin, K.M. and Zhang, G.Y. (2006), "Study on dynamics characteristics of concrete floating slab track in urban track", *Key Eng. Mat.*, **302-303**, 700-705.

Ju, S.H. (2013), "Improvement of bridge structures to increase the safety of moving trains during earthquakes", *Eng. Struct.*, **56**(11), 501-508.

Ju, S.H. and Li, H.C. (2011), "Dynamic interaction analysis of trains moving on embankments during earthquakes", *J. Sound Vib.*, **330**(22), 5322-5332.

Kalker, J.J. (1967), *On the rolling contact of two elastic bodies in the response of dry friction*, Delft University of Technology, The Netherlands.

Li, D.Q., Bilow, D. and Sussmann, T. (2010), "Slab track for shared freight and high speed passenger service", *Joint Rail Conference*, *Proceedings of the 2010 Joint Rail Conference*, Urbana-Champaign, USA, April.

Liu, F.S., Zeng, Z.P., Wu, B., Zhang, Z.C. and Peng K. (2014), "Study of the effect of cement asphalt mortar disease on mechanical properties of CRTS II slab ballastless track", *Adv. Mater. Res.*, **906**, 305-310.

Lin, J.H., Zhang, W.S. and Williams, F.W. (1994), "Pseudo-excitation algorithm for non-stationary random seismic responses", *Eng. Struct.*, **16**(4), 270-276.

Lou, P. and Zeng, Q.Y. (2005), "Formulation of equations of motion of finite element form for vehicle-track-bridge interaction system with two types of vehicle model", *Int. J. Numer. Meth. Eng.*, **62**(3), 435-474.

Lu, F., Gao, Q., Lin, J.H. and Williams, F.W. (2006), "Non-stationary random ground vibration due to loads moving along a railway track", *J. Sound Vib.*, **298**(1-2), 30-42.

Lu, F., Lin, J.H., Kennedy, D. and Williams, F.W. (2009), "An algorithm to study non-stationary random vibrations of vehicle-bridge systems", *Comput. Struct.*, **87**(3-4), 177-185.

Majka, M. and Hartnett, M. (2009), "Dynamic response of bridges to moving trains: A study on effects of random track irregularities and bridge skewness", *Comput. Struct.*, **87**(19-20), 1233-1252.

Miyamoto, T., Ishida, H. and Matsuo, M. (1997), "Running safety of railway vehicle as earthquake occurs", *Q. Rep. RTRI*, **38**(3), 117-122.

Nigam, N.C. (1983), *Introduction to Random Vibration*, MIT Press, Cambridge, MA, USA.

Sogabe, M., Ikeda, M. and Yanagisawa, Y. (2007), "Train-running quality during earthquakes and its improvement for railway long span bridge", *Q. Rep. RTRI*, **48**(3), 186-189.

Wu, Y.S. and Yang, Y.B. (2003), "Steady-state response and riding comfort of trains moving over a series of simply supported bridges", *Eng. Struct.*, **25**(2), 251-265.

Xia, H., Han, Y., Zhang N. and Guo, W.W. (2006), "Dynamic analysis of train-bridge system subjected to non-uniform seismic excitations", *Earthq. Eng. Struct. Dyn.*, **35**(12), 1563-1579.

Xia, H. and Zhang, N. (2005), "Dynamic analysis of railway bridge under high-speed trains", *Comput. Struct.*, **83**(23-24), 1891-1901.

Yang, Y.B. and Wu, Y.S. (2002), "Dynamic stability of trains moving over bridges shaken by earthquake", *J. Sound Vib.*, **258**(1), 65-94.

Yang, Y.B., Yau, J.D. and Wu, Y.S. (2004), *Vehicle-bridge Interaction Dynamics: with Applications to*

High-speed Railways, World Scientific, Singapore.

Yau, J.D. (2009), "Response of a train moving on multi-span railway bridges undergoing ground settlement", *Eng. Struct.*, **31**(15), 2115-2122.

Zhai, W.M. and Cai, C.B. (2002), "Train/track/bridge dynamic interaction: simulation and applications", *Vehicle Syst. Dyn.*, **37**(l), 653-665.

Zhang, N., Xia, H., Guo, W.W., Zhan, J.W., Yao, J.B. and Gao, Y.M. (2010b), "Vehicle-bridge interaction analysis of heavy load railway", *Procedia Eng.*, **4**, 347-354.

Zhang, Z.C., Lin, J.H., Zhang, Y.H., Zhao, Y., Howson, W.P. and Williams, F.W. (2010a), "Non-stationary random vibration analysis for train-bridge systems subjected to horizontal earthquakes", *Eng. Struct.*, **32**(11), 3571-3582.

CC